Experimental Investigation of Biofilter Parameters

by

Shahid Majeed Azam

A Thesis Presented to the

FACULTY OF THE COLLEGE OF GRADUATE STUDIES

KING FAHD UNIVERSITY OF PETROLEUM & MINERALS

DHAHRAN, SAUDI ARABIA

In Partial Fulfillment of the
Requirements for the Degree of

MASTER OF SCIENCE

In

CHEMICAL ENGINEERING

June, 1996

EXPERIMENTAL INVESTIGATION OF BIOFILTER PARAMETERS

BY

SHAHID MAJEED AZAM

A Thesis Presented to the

FACULTY OF THE COLLEGE OF GRADUATE STUDIES

KING FAHD UNIVERSITY OF PETROLEUM & MINERALS

DHAHRAN, SAUDI ARABIA

In Partial Fulfillment of the
Requirements for the Degree of

MASTER OF SCIENCE

In

CHEMICAL ENGINEERING

JUNE 1996

KING FAHD UNIVERSITY OF PETROLEUM & MINERALS
DHAHRAN, SAUDI ARABIA

This Thesis written by

Shahid Majeed Azam

under the direction of his Thesis Advisor, and approved by his Thesis Committee, has been presented to and accepted by the Dean, College of Graduate studies, in partial fulfillment of the requirements for the degree of

MASTER OF SCIENCE IN CHEMICAL ENGINEERING

Thesis Committee:

Chairman (Dr. Shareefdeen M. Zarook)

Co-Chairman (Dr. Abdulla A. Shaikh)

Member (Dr. Adnan M. Jarallah Al-Amer)

Dr. Dulihan K. Harbi
Department Chairman

Dr. Ala H. Rabeh
Dean, College of Graduate Studies

Date: 25/8/96

DEDICATED

TO

MY PARENTS

Acknowledgment

First and foremost, I thank the Almighty, who gave me the opportunity, courage and patience to carry out this work.

Acknowledgment is due to King Fahd University of Petroleum and Minerals for providing support to this work. I would also like to acknowledge the Chairman of the Chemical Engineering Department, Dr. Dulihan K. Harbi for allowing me to use the computing facilities of the department.

I am indebted to my thesis committee Chairman, Dr. Shareefdeen M. Zarook, for his invaluable support, continuous guidance and encouragement, advice and kind helps he extended to me during the course of this work. I also extend my grateful thanks to my thesis committee Co-Chairman, Dr. Abdulla A. Shaikh, for his constant encouragement, invaluable suggestions and advice that have contributed tremendously to the success of this thesis. I also gratefully acknowledge the suggestions and comments by Dr. Adnan M. Jarallah Al-Amer to improve the work.

My sincere thanks are due to Mr. Abdul Appa for allowing me to use the facilities of the Environmental Engineering laboratory. I also thank Mr. John Chapman for constructing the experimental setup in a relatively shorter time. My thanks are due to Mr. Mariano Gica, Mr. Kamal Ahmed, Mr. Basheer Ahmed and Mr. Romeo for their kind help and support.

My sincere appreciation to my friend Mr. Salman Naqvi for his wonderful support in computer work. I would also like to thank the rest of my friends for their help and company that made my stay on campus eminently enjoyable.

Finally a word of grateful thanks to my parents who never shackled my freedom and gave me unstinted support and unlimited discretion in pursuing what I thought best.

Table of Contents

List of Figures

List of Tables

NOMENCLATURE

A_s : biolayer surface area per unit volume of the reactor (m^{-1})

C : dimensionless concentration of tracer, defined as C_i / C_{pulse}

C_i : concentration of tracer at the exit, g m^{-3}

C_j : concentration of pollutant j in the air at a position h along the biofilter (g m^{-3})

C_{je} : value of C_j at h = H (g m^{-3})

C_{ji} : value of C_j at h = 0 (g m^{-3})

C_o : oxygen concentration in the air at a position h along the biofilter (g m^{-3})

C_{oi} : oxygen concentration in the air at the inlet of the biofilter (g m^{-3})

C_{pulse} : concentration of tracer as a pulse input to the system, (g m^{-3})

$\overline{C}_j$: dimensionless concentration of pollutant j in the air

$\overline{C}_o$: dimensionless concentration of oxygen in the air

d_p : diameter of the particle of packing material (m)

D : dispersion coefficient in the vessel ($m^2 h^{-1}$)

D_{JA} : diffusion coefficient of pollutant j in air ($m^2 h^{-1}$)

D_{jw} : diffusion coefficient of pollutant j in water ($m^2 h^{-1}$)

D_{ow} : diffusion coefficient of oxygen in water ($m^2 h^{-1}$)

$E(t)$, E_i : exit age distribution of the tracer leaving the vessel

f_p : friction factor

$f(X_v)$: ratio of diffusivity of a compound in the biofilm to that in water

h : position in the column (m) ; h = 0 at the entrance, h = H at the exit

H : total height of the biofilter bed (m)

K_j : constant in the specific growth rate expression of a culture growing on compound j (g m^{-3})

K_{Ij} : inhibition constant in the specific growth rate expression of a culture growing on compound j (g m^{-3})

K_o : constant in the specific growth rate expression of a culture, expressing the effect of oxygen (g m^{-3})

m_j : distribution coefficient for the substance j/water system

m_o : distribution coefficient for the oxygen-in-air/water system

Pe : Peclet number for the reactor

ΔP : pressure drop (m of water)

R' : relative value of removal rate

Re_p : particle Reynold number

R_{exp} : experimentally measured removal rate of compound j, based on the entire biofilter (g m^{-3}-packing h^{-1})

R_{model} : model predicted removal rate of compound j, based on the entire biofilter (g m^{-3}-packing h^{-1})

S_j : concentration of pollutant j at a position x in the biolayer at a point h along the column (g m^{-3})

$\bar{S}_j$: dimensionless concentration of substance j at a point θ in the biolayer

S_o : oxygen concentration at a position x in the biolayer, at a point h along the column (g m^{-3})

$\bar{S}_o$: dimensionless concentration of oxygen at a point θ in the biolayer

t, t_i : time at which tracer measurements were taken at exit (min)

Δt_i : time interval between measurement of tracer (min)

t_m : mean residence time (min)

U_g : superficial air velocity in the biofilter; (m h^{-1})

X_v : biofilm density (g-dry cells m^{-3})

x : position in the biolayer (m)

x_{H2O} : moisture content in the bed

Y_j : yield coefficient of a culture on VOC j (g-biomass g^{-1}-compound j)

Y_{oj} : yield coefficient of a culture on oxygen (g-biomass g^{-1}-oxygen), when VOC j is the carbon source

Z : dimensionless position in the biofilter (z = h/H)

Greek Symbols

γ : inverse dimensionless inhibition constant defined as $\gamma = K_j / K_{Ij}$

δ : effective biolayer thickness (m)

δ^* : actual biolayer thickness (m)

ε_1 : dimensionless quantity

ε_2 : dimensionless quantity

θ : dimensionless position in the biolayer defined as x/δ

λ : dimensionless quantity

μ_r : viscosity of the fluid (kg m^{-1} s^{-1})

μ : specific growth rate (h^{-1})

μ_j^* : constant in the specific growth rate expression (h^{-1})

η : dimensionless quantity

ϕ^2 : dimensionless quantity

τ : space-time (h)

υ : porosity of the biofilter bed

ρ : density of fluid (kg m^{-3})

ω : dimensionless quantity

σ^2 : variance

σ_θ^2 : normalized variance

Θ : dimensionless time defined as t_i / t_m

THESIS ABSTRACT

NAME OF THE STUDENT	Shahid Majeed Azam
TITLE OF THE STUDY	Experimental Investigation of Biofilter Parameters
MAJOR FIELD	Chemical Engineering
DATE OF DEGREE	June, 1996

Biological destruction of toluene vapor from air streams was studied in a laboratory scale biofilter. The packing material (peat) used in the reactor was immobilized with acclimatized bacterial suspension. The original microbial consortium was obtained as an activated sludge suspension from a local waste water treatment plant. A detailed analysis of the residence time distribution (RTD) was performed under abiotic condition. The RTD results showed that there is significant amount of dispersion in the biofilter. Moisture of the bed, being one of the most important operational parameter, was varied to see the change in the removal of the toluene vapor. It was found that the biofilter works efficiently around 50% moisture content. Pressure drop observed in the biofilter was different than the calculated values through Ergun equation. Correlations were obtained for the biolayer surface area and the porosity with respect to moisture content. Different sets of experiments were also performed to see the effect of oxygen concentration on the removal of the toluene. The effect of oxygen was studied at the inlet concentration of toluene ranging from 1.5 g m^{-3} to 17.5 g m^{-3}. At higher concentration of polluted stream the effect of oxygen was more significant. An axial dispersion model had been developed and the equations were solved using orthogonal collocation technique. The predicted concentration profiles were in excellent agreement with the experimental data. A sensitivity analysis of the model revealed the key parameters which were significant in the operation of biofilters.

MASTER OF SCIENCE

KING FAHD UNIVERSITY OF PETROLEUM & MINERALS

Dhahran, Saudi Arabia

June, 1996

خلاصة الرسالة

الاسم : شاهد مجيد أعظم

عنوان الرسالة : دراسة تجريبية عن معالم مفاعلات التصفية الحيوية

التخصص : الهندسة الكيميائية

تاريخ الشهادة : محرم ١٤١٧هـ

تقدم هذة الرسالة دراسة تجريبية عن التخلص الحيوى من بخار مادة التولوين الموجود في الهواء باستخدام مفاعل تصفية حيوية معملي. استخدم في هذا المفاعل مهد من مادة الخث ثبت فى مكانه عن طريقة تغطيته بطبقة بكتيرية متأقلمة، و قد حصلنا على خليط الطبقة البكتيرية الأصلى كوحل من أحد معامل معالجة مياه الصرف الصحي المحلية.

أجريت فى البداية تجارب مستفيضة لدراسة توزيع زمن الاقامة فى المفاعل (RTD)، تحت ظروف غير حيوية. و بينت هذة التجارب وجود مقدار كبير من الانتشار المادى داخل المفاعل. كما أجريت كذلك تجارب أخرى لدراسة تأثير رطوبة المهد على أداء المفاعل من ناحية القدرة على التخلص من مادة التولوين، و بينت هذة التجارب أن المفاعل يعمل بفاعلية أكبر عند ما تكون نسبة الرطوبة ٥٠٪. لقد أجريت بالأضافة الى ما تقدم مقارنة هبوط الضغط المقاس معمليا فى المفاعل بالقيم المحسوبة بأستخدام معادلة "Ergun" المشهورة، و وجد أن هناك اختلافا بين القيم المقاسة و تلك المحسوبة بالمعادلة.

بعد ذلك أجريت تجارب مستفيضة عن تأثير تركيز الأكسيجين على التخلص من التولوين و ذلك بأستخدام المجال التالي لتركيز الأكسيجين : ١,٥-١٧,٥ غرام / متر^{٣} و بينت هذة التجارب ان الأكسيجين أكثر تاثيرا عند التركيز العالي لمادة التولوين.

ختاما طور في هذة الرسالة نموذج رياضى للمفاعل يأخذ في الاعتبار أنتشار المادة المحورى، و تم حل معادلات النموذج بأستخدام الحاسوب. عند مقارنة تركيز المواد المتفاعلة على امتداد ارتفاع المفاعل التى حصلنا عليها عن طريق هذا النموذج مع تلك التى وجدت تجريبيا وجدنا النموذج يعطى نتائج ممتازة. كما أستخدم هذا النموذج لدراسة حساسية اداء المفاعل لأهم المعالم التشغيلية.

درجة الماجستير في العلوم

جامعة الملك فهد للبترول و المعادن

الظهران ، المملكة العربية السعودية

Chapter 1

Introduction

Increasing stringent regulations concerning public health and of course a growing involvement of mankind in environmental problems have resulted in paying more attention to the environmental aspects of industrial processes. One of these environmental aspects concerns the treatment of the waste gases, which contain odorous organic components. These components may be a mere source of nuisance or may directly endanger health, depending on their nature. As a result of statutory control of air pollution being enforced in many countries, small factories and industries are in want of simple, inexpensive and reliable waste gas cleaning techniques. Driven by this tightening limits on odors and air pollution, intense research efforts are underway in many countries around the world.

The single largest environmental challenge facing the chemical process industries (CPI) today is the control of volatile organic compounds (VOCs). VOCs may be used as feedstock in synthesis or may even be present in final products such as

gasoline. They are also used in small factories such as lacqueries and paint shops. The publicly owned wastewater treatment plants are also a significant source of air emissions of VOCs. Owing to their large volatility, VOCs are of concern due to possible health impacts on humans, as well as a source of reactive organic gases in ozone non-attainment zone. Various technologies have been used for years to control the emissions of VOCs discharged from point sources. The most common are incineration, carbon adsorption and washing in packed-bed columns (Bohn, 1992). Of these methods, incineration only achieves complete destruction of VOCs but requires large amounts of supplemental fuel since the VOC concentration in industrial process vent-streams is too low to provide for self-sustaining combustion (McInnes *et. al.*, 1990). In addition, incineration also produces NO_x gases. Carbon adsorption is an effective method but it is costly requiring either regeneration or transportation of the saturated carbon to a hazardous waste landfill. Water washing is ineffective for VOC treatment because it removes only water soluble gases. Adding acids or bases is also ineffective for VOCs, but may enhance the removal of volatile inorganic compounds (Bohn, 1992). Despite the approaches, described above, being unsatisfactory for treating air with low pollutant concentration, it treats a wide variety of pollutants at high concentrations (Hodge *et. al.*, 1993).

A number of research efforts have focused on the use of biological means to purify air with low pollutant concentration. Although the concept of using microorganisms for the removal of environmentally undesirable compounds has been well established in the area of wastewater treatment, only recently have biological

technologies been seriously considered for the removal of pollutants from other environmental media. Bioremediation techniques are now being successfully applied for the treatment of contaminated soil. It is also hoped that biological systems for the control of air contaminants would prove to be more cost effective technology in the near future.

A recent development in the use of biological processes for air pollution control which has attracted a lot of attention is biofiltration. Biofiltration utilizes microorganisms immobilized on a porous solid material (e.g. peat, perlite, compost, ceramic particles) to degrade pollutants into water, carbon dioxide, and other inorganic constituents. This process is expected to be effective only at low concentrations which are characteristics of emissions. The vessel in which biofiltration takes place is called a biofilter. As a gas stream passes through a biofilter the pollutants are transported into a liquid biolayer surrounding the porous substrate particles, and oxidized (i.e. degraded). Compared to conventional air pollution control techniques (e.g. incineration, washing, adsorption) biofiltration offers a number of advantages: it is relatively harmless to the environment because it does not transfer pollutants to other media, it is inexpensive since it uses natural packing material, and it operates at ambient temperature (Dharmavaram, 1992). Biofilters are of different types, the biotrickling filters or bioscrubbers operate with a recirculating liquid phase, whereas the classical biofilters do not have a continuous liquid phase. In classical biofilters, the required moisture is provided by prehumidifying the air stream and/or by supplying water occasionally (Togna and Singh, 1994).

Biofiltration has been used for many years for odor control (H_2S, and related sulfur compounds, esters, etc.,) in different countries, especially in Europe. The use of biofilters to degrade more complex volatile emissions from chemical plants has started a decade ago by Ottengraf and his coworkers in the Netherlands(Ottengraf and van den Oever, 1983).

A mathematical model, subject to certain assumptions, represents one or more aspects of the physical system. Although a model cannot exactly represent the reality of a system, the behavior of the model predictions can be very close to the responses of the system. Moreover, models have become powerful in decision making processes as they can be used to predict the behavior of the system under shock loading conditions. Some models have been reported in the literature to represent the biofiltration process. A very simplistic model (Ottengraf and van den Oever, 1983) which assumes zero order or first order kinetics and more rational models (Zarook *et. al.*, 1993) have been developed. But in view of developing biofiltration technology more detailed mathematical models are to be developed with lesser constraints.

The present study was undertaken to develop and experimentally verify a detailed model of biofiltration. A detailed model describing steady state operation of a biofilter has been developed, numerically solved and experimentally validated. Biofiltration experiments was performed in a small scale biofilter (5cm diameter, 65cm high). Peat was used as a packing material. The microbial consortium obtained from a wastewater plant was immobilized on the packing material. Experimental validation of the models was based on data obtained from biofiltration of toluene

vapor. Toluene, also a hydrophobic compound, is a priority environmental pollutant. It serves as feedstock for synthesis and is also a substantive constituent of gasoline. As opposed to approaches taken by other researches, this study took into account the mixing characteristics of the fluid in the biofilter. The mathematical model not only included the dispersion term but was also verified experimentally through RTD analysis. Although the effect of oxygen was considered by Zarook *et. al.* (1993) in their model, but there had been no experimental verification of the potential limiting effects of oxygen on the process. This study also undertakes to verify the effect of oxygen experimentally. Many researchers (Leson and Winer,1991; Ottengraf and van den Oever, 1983) have stressed the importance of moisture content in the biofilter beds as moisture is very essential for the survival and metabolism of the microorganisms. However, the effect of varying moisture content in the bed has never been systematically studied experimentally. The present work also includes the study of the effect of moisture on the biofiltration performance experimentally.

As it will be clear from the analysis of the literature review (chapter 2), the objectives of the thesis are as follows:

1. Most theoretical studies on biofilters have assumed plug flow behavior of the fluid which may not be true. The porous nature of the packing material used in biofilters could lead to significant dispersion. Moreover, the occasional sprinkling of water can cause formation of lumps, stagnant zones or channeling effects. The above mentioned factors could deviate the behavior of fluid from the idealized plug flow. To explore the

mixing characteristics in a biofilter a detailed experimental analysis of the residence time distribution was performed.

2. The aerobic bacteria present in the biofilter also requires oxygen to survive. For low concentration of the contaminated waste gases, the oxygen present in the air may prove to be in excess however, at higher concentrations the oxygen could become limiting. As the second objective, the effect of oxygen on the removal of VOCs was studied experimentally and theoretically.

3. Moisture is one of the most critical operational parameter for an efficient biofilter. Low moisture content would quickly dry out the bed reducing microbial activity. At high moisture contents there could be formation of lumps and anaerobic zones. As the next objective, effect of moisture content on the removal was determined experimentally.

4. A steady state model was developed taking into account the axial dispersion effects. This model was used to validate and analyze the data for various conditions as stated in objectives 1 to 3.

Chapter 2

Literature Survey

2.1 Biofiltration

2.1.1 Introduction

Biofiltration is an adaptation of the process by which the atmosphere is cleaned naturally. Plants and soils adsorb the VOC existing in the atmosphere and degrade them. Although this process has been going on for a great number of years, it is inefficient, due to limited contacts of plants and soils with the atmosphere and slow reaction rate (Bohn, 1992). Another reason for its inefficiency could be the massive increase in the synthesis of organic chemicals. Many of these chemical compounds are xenobiotic or foreign to the already existing soil microorganisms and as a result are not degraded. Consequently, they accumulate in the environment which could pose a serious threat to human health. Biofiltration technology could be used commercially to reduce the emissions of such harmful organic compounds. This technology provides

maximal contact and allows sufficient time for the pollutants to be degraded either by microbial consortium present in the activated sludge suspension or by genetically altered microorganisms. Biofiltration has had more industrial success for treating malodorous emissions, but is also expected to be very promising for control of solvent emissions.

Treatment of odorous gases by biological methods can be found in literature as early as 1920s. The first biofilter was patented in the US by Pomeroy in 1957, which consisted of slotted pipes buried under a soil. These were called 'open earth filters' and utilized natural microorganisms. Such soil filter beds were unsuccessful due to the requirement of large land area, poor air distribution and inefficient moisture control (Dharmavaram, 1993). The other type of biofilters used for control of malodorous emissions was a closed packed tower design which consisted of an organic packing media. These biofilters do not require as much space as earth filters and the temperature and humidity can be effectively controlled.

Biofiltration for the elimination of the volatile organic emissions in biotowers has been first explored by Ottengraf and his associates in 1983. These researchers evaluated the performance of inoculated compost as a filter bed medium in the treatment of toluene, butyl acetate, ethyl acetate and butanol emitted from lacqueries. A theoretical model representing the processes in a biofilter was also presented by these authors.

2.1.2 Filter material and microorganisms

For a biofilter to operate efficiently the filter material must have several qualities. The most important is that it must provide hospitable environment (i.e. O_2, moisture, temperature, nutrients and pH) for the microbial population to achieve high degradation rates. Second, filter particle size distribution and pore structure should provide large reactive surface area and low pressure drop (Leson & Winer, 1992). Third, the filter media must exhibit minimum bed compaction.

Since peat and compost provide favorable conditions for microbes, they are used as basic filter material. Other materials such as porous clay or polystyrene spheres are sometimes added to increase reactive surface durability and decrease the pressure drop. Activated carbon can be used to increase the filter's buffer capacity.

Several groups of microorganisms are known to be involved in the degradation of the air pollutants in biofilters, primarily bacterial species. Naturally occurring media such as peat and compost contain roughly one billion microorganisms per gram, capable of degrading some pollutants. Introduction of organic off-gases into the biofilter will generally shift the distribution of the existing microbial populations towards strain that metabolize the target pollutants. For easily biodegradable organic compounds, acclimation will typically take 10 days (Ottengraf, 1986). For less biodegradable compounds, an appropriate culture has to be inoculated. Activated sludge suspensions from sewage treatment plants can serve as inoculum (Ottengraf and Diks, 1990) in some cases, but more poorly biodegradable compounds such as

chlorinated hydrocarbons and aromatics require inoculation with specially cultivated organisms (Ottengraf *et. al.* 1986; Ottengraf and Diks, 1990).

Most industrial sources of air pollutants do not operate continuously, hence it was of interest whether biological activity suffered during shut down periods. Results reported by Ottengraf and van den Oever (1983) suggest that biofilter beds can survive periods of at least two weeks without any significant reduction in microbial activity. The operation of a biofilter resulting in the contamination of the treated air was studied by Ottengraf and Konings (1986). The authors report that the concentration of the microorganisms in air streams exiting biofilters is only slightly higher than that encountered in the open air.

2.1.3 Moisture content

One of the major operational requirement for a biofilter is the maintenance of an optimum moisture content in the filter material. Moisture content is very essential for the microbiological activity. In case of classical biofilters, the water phase is fixed in the reactor thereby reducing the cost of an extra pump. Although the water phase is fixated, it can leave through evaporation. The gas which passes the reactor at high volumetric flow rates picks up part of the water and thereby dries out the filter bed (van Lith, 1989). To avoid this problem, the contaminated air streams are saturated with water or steam so that they can take no more water. However, the use of steam can lead to a temperature rise thus reducing the biological activity (van Lith *et. al.*, 1990). Even with prehumidification, the filter bed gets dried up in some cases. This is

due to the fact that biodegradation is an exothermic oxidative process. A logical solution to this problem is sprinkling the filter bed with water. But this in fact has two major disadvantages. The formation of anaerobic zones (Ottengraf *et. al*, 1983) and the possibility of creation of lumps leading to decrease in the components interchanging surface. The drying out of filter bed creates fissures leading to channeling effects. The decrease in the detention time due to short circuiting considerably reduces the removal rates.

2.1.4 Oxygen

The aerobic heterotrophic bacteria present in the classical biofilter requires oxygen to survive. Many researchers (Ottengraf & van den Oever, 1983; Dharmavaram, 1991; Bohn, 1993) have assumed that the oxygen is in excess for biofiltration of VOCs. Zarook *et. al.*, (1993), in a theoretical model, used expressions for the reaction rate which explicitly took into account the potential limiting effect of the oxygen. However, they did not report any experimental results for the effect of oxygen. Diks (1992) suggested that a continuos supply of oxygen in the gas phase may be required by the trickling biofilter. However, the problem of oxygen availability has not been explored experimentally.

2.1.5 Nutrients supply & pH control

Microorganisms apart from requiring oxygen and a carbon source, also require inorganic nutrients such as nitrogen and phosphorus to survive. The natural occurring

packing materials such as peat, compost, and bark when used as filter substrate supply the nutrients necessary to support the growth and survival of the microorganisms. Lysis of cells also leads to release of nutrients. In some cases however, depending on the target pollutant and the source of the filter material, the availability of specific nutrients might become process limiting. For example, the addition of nutrients to a biofilter material has been shown to improve the biodegradation of some compounds significantly (Don, 1985). In case of biotrickling filter and bioscrubbers, external nutrients are supplied.

The microbial activity is strongly affected by a drift from a preferable pH range. Biodegradation of sulfur, nitrogen or halogen containing compounds leads to the formation of acids which lowers the pH. The acidification of the filter bed restricts the treatment of such compounds in biofilters. Biological systems using liquid phase (e.g. bioscrubbers and biotrickling filters) allow for a much easier pH control. Water stream is easily neutralized before recirculating it through the reactor (Diks, 1992; Diks and Ottengraf, 1991; Oh, 1993). These biological systems have therefore been considered for the treatment of off-gases containing high loads of acidic degradation products. Higher concentration of neutralization products such as NaCl and $CaCl_2$ have been reported to inhibit the microbial activity.

2.1.6 Temperature effect and pressure drop

The typical range for efficient biofilter operation is between 5 to 50°C. Temperature higher than the above limit kills the bacteria and lower temperature

inactivates them. In some cases the degradation rates typically increase with temperature. Arrhenius expression can be used to describe the effect of temperature on degradation over certain ranges (Zilli *et. al.*, 1993). An increase in temperature by 7°C has experimentally shown to increase the elimination capacity of a styrene eliminating biofilter by a factor of approximately 2 (Ottengraf and Diks, 1990).

Due to gradual compaction of the natural packing material the pressure drop will increase with time. However, a number of studies have shown that the pressure drop in a biofilter is very low. The values reported (Deshusses and Hamer, 1993; Sorial *et. al.*, 1993) are around 1 to 2 inches water per meter of filter bed. The compaction can be minimized by adding certain materials such as bark and polystyrene spheres (Dharmavaram, 1991). External addition of water also increases the pressure drop (Ottengraf and Diks, 1990). This can be explained as the surface irrigation at the top of the biofilter bed clogs the pores of the packing material.

2.2 Experimental studies on VOC removal in biofilters

Studies on the removal of VOCs was first reported by Ottengraf and van den Oever (1983) who studied the biofiltration of air pollutants from lacqueries which constituted mixtures of butyl acetate, ethyl acetate, toluene and butanol. It has been reported by these authors that a period of fortnight can be spanned with hardly any loss in the microbial activity. This finding is important for the cases where there is a discontinuous release of the VOCs. Hodge et. al (1991) examined the effect of

different packing material on the removal of jet fuel and diesel fuel vapors. Zilli *et. al.* (1993), in their study of removal of phenol vapors from waste gases in the classical biofilter, obtained 93-99% conversion even at moderate phenol concentrations. Biological degradation of ethanol emissions, from investment casting and bakery, was carried out by Leson *et. al.* (1993) using a full-scale and pilot-scale biofilters. A bench scale vapor phase biological reactor with fully computerized data acquisition system was used by Phipps and Ridgeway (1993) to biofilter gasoline fractions. Ergas *et. al.* (1993) have removed chlorinated compounds and toluene in a classical biofilter. Despite using chlorinated compounds as target pollutants a classical biofilter was used, but to maintain the pH of the filter media crushed oyster shells, a source of calcium carbonate, was added. A field pilot demonstration study was conducted by Togna and Frisch (1993), to treat plant styrene emissions in a biofilter. Deshusses and Hamer (1993), were successful in removing methyl ethyl ketone (MEK) and methyl isobutyl ketone (MIBK) using a classical biofilter with packing material primarily consisting of clay spheres. Zarook *et. al.* (1993) have successfully removed methanol vapor in a biofilter which contained natural packing material (peat and perlite in the volume ratio of 2:3) inoculated with methanol degrading microorganisms. Zarook and Baltzis (1993), extended the work to study the removal of toluene using the same packing material but inoculated with a culture obtained from a microbiology laboratory of Rutgers University, New Jersey, USA. The removal of low concentration of VOCs present in the waste air streams of Publicly Owned Treatment Works (POTWs) was studied by Torres *et. al.* (1994). Bench scale experiments were used to test the

effectiveness of biofiltration in treating air contaminated with ethanol vapors by Hodge and Devinny (1994). Biofiltration has also proved to be successful for the removal of inorganic emissions (Barnes *et. al.*, 1995).

2.3 Modeling studies on biofiltration process

Steady state models representing the biofiltration process have been first described by Ottengraf and van den Oever (1983). Their model focuses on the steady state biofiltration process which assumes VOCs to be in equilibrium at the air/biolayer interface, plug flow of the gas phase and simple kinetics: zero-order and first-order kinetics. For VOC mixtures the authors proposed to use the same model, which is valid for single VOC removal, in an additive sense. The concept of 'effective biolayer' has also been introduced by Ottengraf and van den Oever (1983). This concept implies that the VOCs are depleted only in a fraction of the biolayer. More recently, kinetic expressions appropriate for biological systems, such as Monod and Andrews inhibitory kinetics, have been explored by Zarook *et. al.* (1993) and Zilli *et. al.* (1993). For modeling the biofiltration of MEK and MIBK mixtures Deshusses and Dunn (1993) have used a competitive kinetic expression. The model of Ottengraf and van den Oever (1983) assumes no oxygen limitation on the biofiltration process. However, the potential limiting effects should be considered and it has been taken into consideration by Zarook *et. al.* (1993), and Zarook and Baltzis (1993).

Chapter 3

Theory

3.1 Residence Time Distribution

The performance of a reactor depends considerably on the mixing characteristics of the fluid. The deviation from the two idealized patterns, plug flow and mixed flow, can have a variety of causes leading to the non-ideality of the flow. The degree of non-ideality can be characterized through residence time distribution (RTD) analysis. The RTD exhibited by the given reactor yields distinctive clues to the type of mixing occurring within it, and is one of the most informative characterizations of the reactor. Although this analysis has been widely used for characterizing chemical reactors it has received less attention in biological processes. This might be due to the fact that bioreaction engineering is relatively in the rudimentary stage when compared to other chemical engineering processes or perhaps due to the added complexity in finding a suitable tracer for the biological systems. An exception is the field of liquid phase

packed bed biological reactors where considerable amount of work has been done to determine the RTD of the fluid (Donald and Daugulis, 1988).

Most theoretical studies (Ottengraf and van den Oever, 1983; Zarook *et. al.*, 1993) on biofilters are based on the assumption of idealized flow pattern, namely plug flow. In actual operation this might not be the case. Deviations from ideal plug flow can be caused by channeling of fluid, by existence of stagnant regions, due to non-uniformity in the packing material and due to the lack of adequate means of distributing the feed.

If a complete velocity distribution profile of the fluid in a vessel is known then the prediction of the behavior of the vessel as a reactor becomes very easy. However, the attendant complexities make it impractical or physically impossible to use this approach in actual systems. Setting aside the complete knowledge of the fluid flow the only thing that is desired is the knowledge of the residence time distribution of the elements of fluid exiting the reactor. The most widely used method to determine the distribution of residence times of fluid exiting the reactor are stimulus-response techniques. In these techniques, a tracer is injected into the fluid entering the system or some other point within the reactor, and the tracer concentration is measured in the effluent stream or some other point downstream within the reactor. An analysis of the response gives the required information. The proper choice of tracer for a given system in RTD analysis is very critical. The tracer should be easily detectable, should not disturb the flow pattern in the vessel, and should have properties similar to those of reacting fluid, so that its behavior honestly reflects the material flowing through the

reactor. For biological systems the tracer should not get metabolized by the microorganisms involved. The two most widely used methods of tracer injection are pulse input and step input.

When an amount of tracer is suddenly injected into the feedstream in very short time then it is called pulse input. The outlet tracer concentration is then measured as a function of time. The effluent concentration-time curve is referred to as the C curve in the RTD analysis. In a step input the tracer is increased by a certain amount and is then kept at this level until the effluent concentration gets steady.

3.1.1 Characterization of RTD

The residence time distribution of the fluid or the exit age distribution for a pulse input, $E(t)$, is defined as

$$E(t) = \frac{C(t)}{\int_0^\infty C(t)dt} = \frac{C_i}{\sum C_i \Delta t_i} \tag{3.1}$$

The RTD like any other distribution function can also be characterized using some mathematical concepts. The two most important characterization of RTD studies are: the first moment of RTD function, $E(t)$, which gives the mean residence time, t_m, (equation 3.2) and the second moment about the mean, which gives the variance, σ^2, (equation 3.3).

$$t_m = \int_0^\infty tEdt = \sum t_i E_i \Delta t_i \tag{3.2}$$

$$\sigma^2 = \int_0^\infty (t - t_m)^2 Edt = \sum (t_i - t_m)^2 E_i \Delta t_i \tag{3.3}$$

One of two approaches, viz. tank-in-series model and dispersion model, is usually followed to model the non-ideality of the tubular reactor. In the dispersion model, there is an axial dispersion of the fluid resulting from molecular and turbulent diffusion. In dimensionless form, the basic equation representing the model describes mass balance of the tracer as follows :

$$\frac{\partial C}{\partial \Theta} = \frac{1}{Pe}\frac{\partial^2 C}{\partial Z^2} - \frac{\partial C}{\partial Z} \tag{3.4}$$

where Pe is the reactor Peclet number defined as $Pe = \frac{U_g H}{D\upsilon}$. For small extents of dispersion, solution to equation (3.4) gives a symmetrical C curve

$$C(\Theta) = \frac{1}{2\sqrt{\frac{\pi}{Pe}}}\exp[-\frac{(1-\Theta)^2 Pe}{4}] \tag{3.5}$$

which represents a family of gaussian curves with mean and variance as

$$\sigma_\theta^2 = \frac{\sigma^2}{t_m^2} = \frac{2}{Pe} \tag{3.6}$$

$$\Theta = \frac{t_i}{t_m} \tag{3.7}$$

For large extents of dispersion, it has not been possible to obtain analytical expressions for C curves except for the case of open vessels. A schematic of closed-closed vessels and open-open vessels are shown in Figure 3.1.1. For a closed-closed vessel, there is plug flow (no dispersion) to the immediate left of the entrance line (h = 0) and to the immediate right of exit line (h = H). However, there is dispersion and reaction between the entrance line and the exit line. In an open-open vessel dispersion occurs both

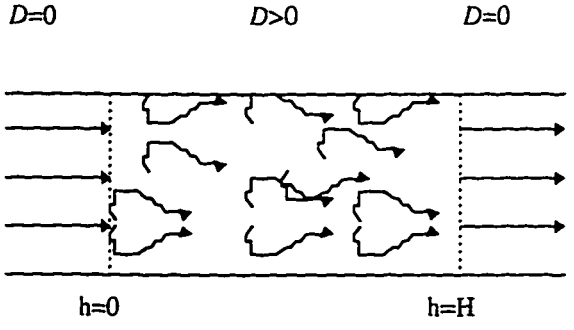

Closed-Closed vessel

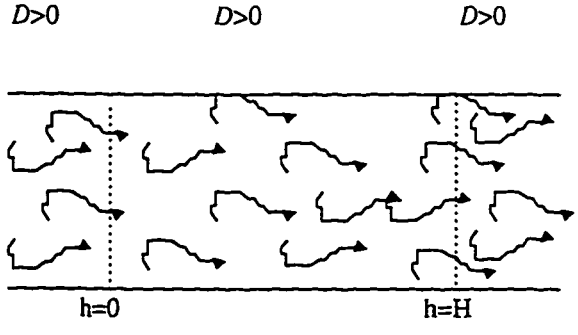

Open-Open vessel

Figure 3.1.1 A schematic of the closed-closed vessel and open-open vessel

upstream (open) and downstream (open) of the reaction section. Van der Laan (1958) has reported the means and variances for many of the cases. The variance for the case of closed-closed vessels (i.e. biofilters) is given as

$$\sigma_{\Theta}^{2} = \frac{\sigma^{2}}{t_{m}^{2}} = \frac{2}{Pe}[1 - \frac{1}{Pe}(1 - e^{-Pe})] \tag{3.8}$$

3.2 Axial Dispersion Model

Models representing the processes of biofilters have been first described by Ottengraf and van den Oever (1983). Their model is based on simplistic assumptions such as zero-order kinetics, availability of excess oxygen, and plug flow of the gas phase. However, more recently kinetic expressions appropriate for biological systems, such as Monod (1932) and Andrews (1968) inhibitory kinetics, have been explored (e.g. Zarook *et. al.* 1993, Zilli *et. al.* 1993). The potential limiting effect of oxygen has also been taken into account by Zarook *et. al* (1993). But to date, most of the models have been based on the assumption of plug flow for the gas phase. Hence, in this work the model of Zarook *et. al.* (1993) is improved by incorporating axial dispersion terms of both VOC and oxygen in the gas phase. These additional terms account for axial mixing in the gas phase. The assumptions made in deriving the model are :

1. The thickness of the biofilm is small compared to main curvature of the solid, hence planar geometry can be used.
2. Biofilm does not grow in the pores of the particles. It is formed only on the exterior surface of the particles.

3. Biofilm might develop on fraction of the total solid surface leaving the bare surface for adsorption.

3. The pollutant and the oxygen are in equilibrium at biofilm/air interface.

5. The depth of penetration of pollutant and oxygen in biofilm is smaller than the actual size of the biofilm. This depth is called the effective biolayer.

6. Biofilm density is constant and specific biofilm surface area is constant for a given moisture content.

7. Diffusivities of the pollutant and oxygen in the biofilm are equal to the diffusivities of the same compounds in water corrected by some factor given by Fan *et. al.* (1990).

A schematic of biofilm model with these assumptions is shown in Figure 3.1.2. Model equations for VOC (j) and oxygen (o) based on the assumptions mentioned above are written as follows:

(I) Mass balances in biofilm :

$$f(X_v)D_{jw}\frac{d^2S_j}{dx^2}-\frac{X_v}{Y_j}\mu(S_j,S_o)=0 \tag{3.9}$$

$$f(X_v)D_{ow}\frac{d^2S_o}{dx^2}-\frac{X_v}{Y_{oj}}\mu(S_j,S_o)=0 \tag{3.10}$$

Boundary conditions :

at x = 0,

$$S_j=\frac{C_j}{m_j} \qquad S_o=\frac{C_o}{m_o} \tag{3.11}$$

at x = δ,

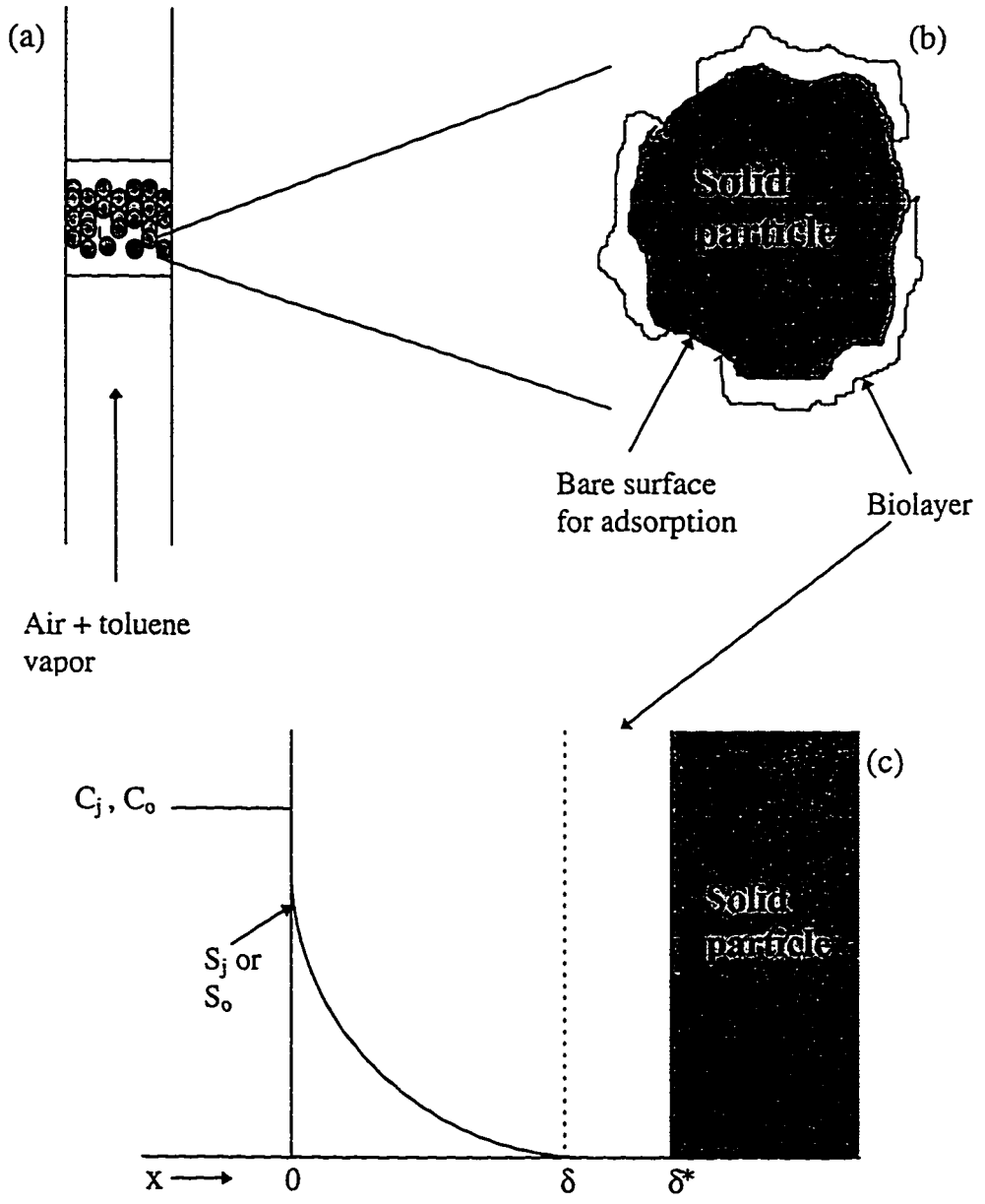

Figure 3.1.2 A schematic representation of the biofilm model. (a) a section from the biofilter. (b) a single particle which is partially covered with biofilm where biological reaction takes place. (c) a section of the biofilm.

$$\frac{dS_j}{dx} = 0 \qquad \frac{dS_o}{dx} = 0 \tag{3.12}$$

(II) Mass balances in the gas phase :

$$\upsilon D\frac{d^2C_j}{dh^2} - U_g\frac{dC_j}{dh} + f(X_v)D_{jw}\left.\frac{dS_j}{dx}\right|_{x=0} A_s = 0 \tag{3.13}$$

$$\upsilon D\frac{d^2C_o}{dh^2} - U_g\frac{dC_o}{dh} + f(X_v)D_{ow}\left.\frac{dS_o}{dx}\right|_{x=0} A_s = 0 \tag{3.14}$$

Danckwert's boundary conditions which account for axial dispersion effects at the inlet and exit conditions are used:

at h = 0,

$$\upsilon D\frac{dC_j}{dh} = U_g(C_j|_{0^+} - C_j|_{0^-}) \tag{3.15}$$

$$\upsilon D\frac{dC_o}{dh} = U_g(C_o|_{0^+} - C_o|_{0^-}) \tag{3.16}$$

at h = H,

$$\frac{dC_j}{dh} = 0 \qquad \frac{dC_o}{dh} = 0 \tag{3.17}$$

Model equations are normalized using the following dimensionless parameters

$$\overline{C}_j = \frac{C_j}{C_{ji}} \qquad Z = \frac{h}{H}$$

$$\overline{S}_j = \frac{S_j}{K_j} \qquad \theta = \frac{x}{\delta}$$

$$\omega = \frac{K_o D_{ow} C_{ji}}{K_j D_{jw} C_{oi}} \qquad \gamma = \frac{K_j}{K_{Ij}}$$

$$\varepsilon_1 = \frac{C_{ji}}{K_j m_{ji}} \qquad \varepsilon_2 = \frac{C_{oi}}{K_o m_o}$$

$$Pe = \frac{U_g H}{D\upsilon} \qquad \eta = \frac{f(X_v) D_{jw} H K_j A_s}{U_g C_{ji} \delta}$$

$$\phi^2 = \frac{X_v \mu^* \delta^2}{f(X_v) D_{jw} K_j Y_j} \qquad \lambda = \frac{D_{jw} K_j Y_j}{D_{ow} K_o Y_{oj}}$$

Mass balances in the biofilm :

$$\frac{d^2\bar{S}_j}{d\theta^2} - \phi^2 \frac{\bar{S}_j}{1+\bar{S}_j+\gamma\bar{S}_j^2} \frac{\bar{S}_o}{1+\bar{S}_o} = 0 \tag{3.18}$$

$$\frac{d^2\bar{S}_o}{d\theta^2} - \phi^2 \lambda \frac{\bar{S}_j}{1+\bar{S}_j+\gamma\bar{S}_j^2} \frac{\bar{S}_o}{1+\bar{S}_o} = 0 \tag{3.19}$$

at $\theta = 0$, $\quad \bar{S}_j = \varepsilon_1 \bar{C}_j \qquad \bar{S}_o = \varepsilon_2 \bar{C}_o$ (3.20)

at $\theta = 1$, $\quad \frac{d\bar{S}_j}{d\theta} = 0 \qquad \frac{d\bar{S}_o}{d\theta} = 0$ (3.21)

Mass balances in the gas phase :

$$\frac{1}{Pe}\frac{d^2\bar{C}_j}{dZ^2} - \frac{d\bar{C}_j}{dZ} + \eta \left.\frac{d\bar{S}_j}{d\theta}\right|_{\theta=0} = 0 \tag{3.22}$$

$$\frac{1}{Pe}\frac{d^2\bar{C}_o}{dZ^2} - \frac{d\bar{C}_o}{dZ} + \eta\varpi \left.\frac{d\bar{S}_o}{d\theta}\right|_{\theta=0} = 0 \tag{3.23}$$

at $Z = 0$, $$\frac{1}{Pe}\frac{d\overline{C}_j}{dZ} = \overline{C}_j - 1 \tag{3.24}$$

$$\frac{1}{Pe}\frac{d\overline{C}_o}{dZ} = \overline{C}_o - 1 \tag{3.25}$$

at $Z = 1$, $$\frac{d\overline{C}_j}{dZ} = 0 \qquad \frac{d\overline{C}_o}{dZ} = 0 \tag{3.26}$$

3.3 Moisture content in the biofilter

For the optimal operation of a biofilter the bacterial flora needs a favorable water content in the bed to which it is attached. In classical biofilters the water phase is fixed in the filter material which is placed in the reactor. This results in small energy consumption, because no pump is required to recirculate the water phase over the reactor. Although the water is fixated in the reactor, it can leave the reactor through evaporation. The gases which pass the reactor pick up a part of water and thereby dry out the filter. Maintaining water balance in the reactor is an important aspect which determines the reliable operation of the biofilters. To ensure the water content of the bed precautions have to be taken.

The evaporation of water can be minimized by saturating the inlet stream. Since the biological oxidation taking place in the reactor is exothermic, there will be heat generation. The temperature rise due to heat generation would lead to evaporation of water from the bed. The heat needed for evaporation of this water causes the filter material to cool down again. To solve the problem of drying, entering streams should be prehumidified and water should be directly added to the bed if needed. Prehumidification would completely saturate the entering gas streams. A water

saturated gas stream cannot take anymore water, therefore the water evaporation from the bed will be minimum. Direct humidification of the bed is another solution but it has several disadvantages. The addition of large amounts of water greatly affects the structure of the filter material and the gas flow resistance. This process eventually leads to the reduction in filter material volume and as well as in surface area because of the development of lumps. The water droplet is also of prime importance. Investigations have shown that small variations in the droplet diameter has great impact on the filter material. A droplet with a diameter smaller than 1mm has no long term influence. The waterload on the filter material is another factor which can influence the performance of the biofilter. High waterloads cause the upperlayer of the filter bed to get flooded since the water cannot be transported fast enough to the lower parts. Due to high water loads the added water can also percolate through the filter material. In such case, the filter material does not gets enough time to absorb water. Moreover, the percolated water can take alongwith it some nutrients and microorganisms thereby reducing the efficiency of the filter material. Addition of water through intermediate sampling ports could avoid the high water loads at the top of the column.

3.4 Availability of oxygen

The aerobic, heterotrophic bacteria present in the filter bed require oxygen in the inlet gas stream to survive. Anaerobic regions develop in the filter bed, if the flow through the bed is not uniform and the supply of oxygen is insufficient, thus killing the aerobic bacteria. The formation of anaerobic zones might start producing foul-smelling

emissions which is not desirable. Such occurrences are common in the filter materials which are non-homogeneous.But, according to some authors (Ottengraf and Van den Oever, 1983; Diks and Ottengraf, 1991; Bohn, 1993) oxygen relations are optimal in biofiltration because the input air contains oxygen in excess and the oxygen is intimately mixed with the VOC. This could be true for hydrophobic compounds (e.g. benzene, toluene etc.) at low inlet concentrations but, at high inlet the oxygen could become process limiting in the biolayer. For the case of hydrophilic compounds, which are not easily biodegradable compounds like methanol, the limiting effect of oxygen could be very prominent even at low concentrations.

The potential limiting effect of oxygen on the process has not yet been investigated experimentally. However, there is one theoretical study (Zarook et. al 1993) which has taken into account effect of oxygen.

Chapter 4

Experimental Apparatus & Procedures

4.1 Material and Apparatus

4.1.1 Chemicals

Toluene (30444, BDH Chemicals Ltd., Poole, England) was used as the VOC to be treated. The chemicals used for media preparation were : $MgSO_4.7H_2O$ (29117, BDH Chemicals Ltd., Poole, England); $(NH_4)_2SO_4$ (10033, BDH Chemicals Ltd., Poole, England); $CaCl_2$ fused, granular (27487, BDH Chemicals Ltd., Poole, England); Na_2PO_4 dibasic anhydrous powder (3828-01, J.T. Baker Inc., Phillipsburg, NJ-08864, USA), KH_2PO_4 monobasic crystal (3246, J.T. Baker Inc., Phillipsburg, NJ-08864, USA), anhydrous $FeCl_3$ (28379, BDH Chemicals Ltd., Poole, England).

4.1.2 Calibration

The standard calibration curves were prepared by injecting known amounts of liquid toluene into sealed serum bottles (148 ml) using a 10 µl liquid syringe (#704, Pat. no. 2933087, Hamilton Co., Reno., Nevada). The bottles were sealed with septa and crimped with aluminum caps. The liquid toluene was allowed to evaporate at room temperature within the closed bottle. Gas samples from different serum bottles were injected into the GC using a 200 µl gas tight syringe (#1001, Pat. no. 3140801, Hamilton Co., Reno., Nevada).

4.1.3 Experimental Setup

The laboratory scale apparatus used for the experimental studies consists of a cylindrical column made of Plexiglas with an inner diameter of 6 cm and a height of 68 cm. The height of the packing material in the column was 65 cm. At the bottom of the column a fine ceramic disperser was fixed to get uniform distribution of the gas stream entering the biofilter. The column had several ports allowing for sampling of the air stream and supplying of the water. A U-tube manometer was attached to record the pressure drop. The packing material used was a commercially available peat.

The biofilter bed was supplied with a humidified air stream containing toluene vapor. Laboratory air was humidified by passing through a closed water tank. A peristatic pump was used to pump air at a lower flow rate through a closed toluene tank. A rotameter was used to vary the concentrations of the inlet solvent vapor by allowing a greater or smaller amount of air through the toluene tank. The humidified air stream and the solvent vapor were mixed to create contaminated air stream. The

contaminated air stream was then fed to the column. Another flowmeter was used at the exit to measure the total air flow rate. A schematic of the setup is shown in Figure 4.1.1.

Toluene concentrations were determined using a Perkin Elmer's Autosystem gas chromatograph. The GC was equipped with a stainless steel column and a flame ionization detector. The operating conditions set were: injector 200°C, column 100°C, and detector 240°C. The carrier gas was helium at a flow rate of 21 ml/min. The retention time of toluene under these conditions was around 2.8 min.

4.2 Preparation of mineral medium

The mineral medium is prepared by adding the following chemicals: $(NH_4)_2SO_4$, 1000 mg/l; $MgSO_4.7H_2O$, 42 mg/l; KH_2PO_4, 42 mg/l; Na_2PO_4, 84 mg/l; $CaCl_2.2H_2O$, 42 mg/l; and $FeCl_3$, 0.8 mg/l (Ottengraf and van den Oever, 1983) to one liter of water. The mineral medium was autoclaved before using in the subsequent experiments.

4.3 Preparation of the biomass

The microbial consortium to be used for the biofiltration experiments was obtained from an activated sludge suspension from a local waste water treatment plant. About 4 ml of the activated sludge suspension was mixed with 40 ml of the mineral medium. Using the loop this solution was streaked onto an agar plate. One microliter of toluene

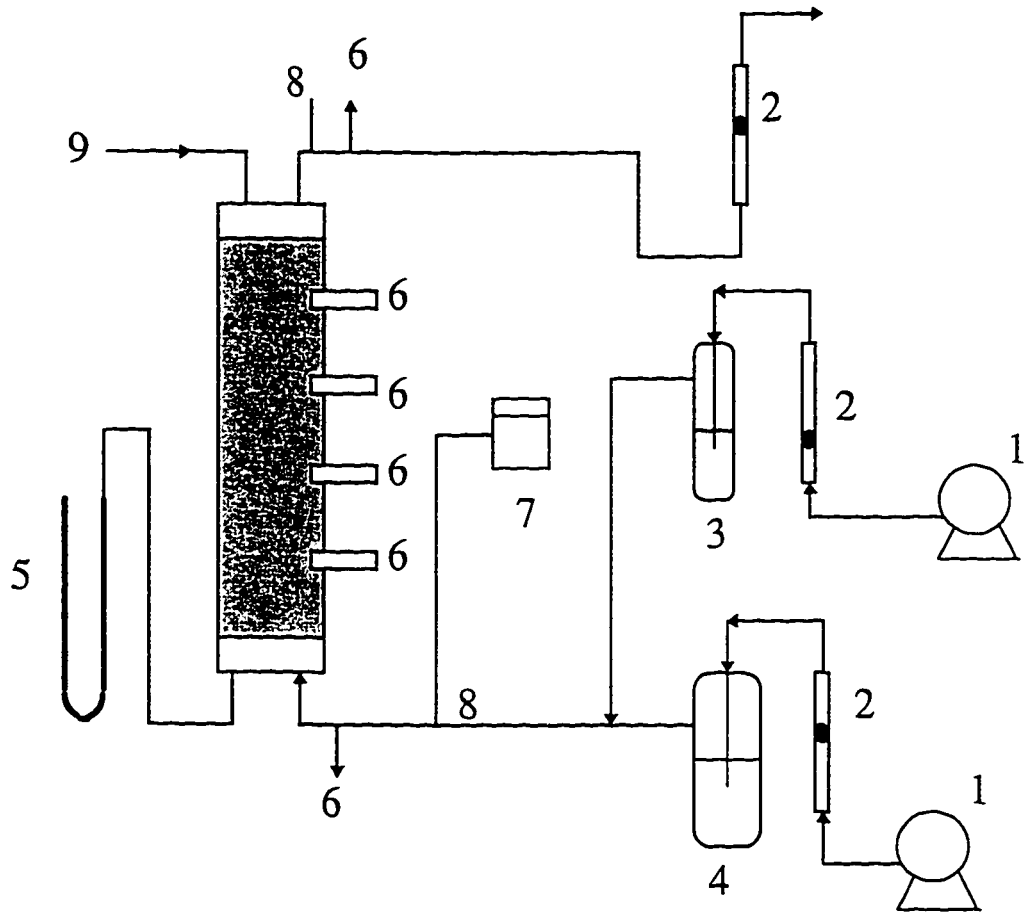

Figure 4.1.1 Schematic of the experimental setup used in this study. 1. Air pump 2. Flow meters 3. Toluene tank 4. Water tank 5. Manometer 6. Sampling ports 7. Humidity and temperature meter 8. Provision for inserting probe 9. Water supply (when needed).

was added on to the plate to serve as the only source of carbon to the microbial consortium. The agar plate was covered and put in an incubator at 30°C for 24 hrs. A loop of dense white colonies of microbes from this agar plate was streaked onto next agar plate and the process was repeated several times. Acclimatized innoculum was then transferred to serum bottles containing fresh mineral medium and toluene as sole carbon and energy source. After significant growth of biomass, content was transferred to a 2 liter biostat (B. Braun, Meisungen AG, Germany, Type 880072, No 198} fermentor. The volume of the suspended suspension was 800 ml providing enough headspace. The suspension was continuously stirred at 140 rpm and external supply of oxygen prevented any oxygen limitations. Toluene was provided at regular intervals for a period of three weeks. The culture was finally centrifuged at 4000 rpm for 14 minutes and concentrated biomass was resuspended in a fresh mineral medium.

4.4 Preparation of the packing material

All the experiments were carried out using peat as the packing material. The selection of peat is based on the discussion available elsewhere (Couillard, 1994). To get an approximately equal size of particles, the peat was sieved with number 20 mesh. The natural packing material contains enough microbes even in the absence of inoculum. The presence of these microorganisms may lead to the production of side products as well as consumption of nutrients present in the natural packing material. To avoid the variations in the microbial activity, the packing material was steam sterilized. The sterilized packing material was mixed with 30% (by volume) of bacterial suspension.

The addition of the bacterial suspension partially filled the pore space with water leaving the other void space for air circulation

4.5 Experimental Procedures

4.5.1 RTD experiments

The setup used for the RTD was same as described above, however, the packing material was damped with 30% (by volume) sterilized medium instead of bacterial suspension. The packed bed was supplied with a humidified air stream containing toluene vapor. An increase or decrease in the concentration of toluene entering the reactor, by varying the flow rates through flow meters (Figure 4.1), allowed us to create tracer input signals. Toluene was selected as tracer as the removal of the same compound was studied. The syringe used for calibration was also used to take samples.

4.5.2 Biofilter experiments

For biofilter experiments the packing was inoculated with the cultured bacterial suspension (30% by volume). Different sets of experiments were carried out by changing the inlet concentration of toluene entering the biofilter.

Since the volume of the biofilter bed under study had a volume of approximately 2 liters, so 600 ml of bacterial suspension was mixed with the packing material to account for 30% moisture content in the bed. To increase the moisture content to 50% another 400 ml of sterilized mineral medium was added. The moisture content of the

bed was further increased to 70% by adding another 400 ml of mineral medium. The mineral medium was added through sampling ports as well as from top of the column. The different oxygen content in the inlet gas was maintained by mixing air with pure oxygen. Oxygen concentrations were analyzed by oxygen analyzer (Servomex, Oxygen Analyser, Serial No. 1184/13) and gas chromatograph (Gow Mac Instrument Co., Series 350). The specification of the column was 6"/8" SS Chrom. The operating conditions set were : injector 140°C, detector 200°C and column 110°C.

Chapter 5

Results and Discussion

5.1 RTD analysis

The experimental data was collected by providing a pulse type of input signal to the system. A sample calculation of RTD data to determine the mean and variance is shown in Table 5.1.1. The **C** curve of the experimental data shown in Table 5.1.1, is given in Figure 5.1.1. The y axis or the C(θ) is calculated as $\frac{E_i}{\sum C_i t_i}$ and θ is calculated as $\frac{t_i}{t_m}$. The mean residence time t_m is obtained by summing up the values of $[t_i E_i \Delta t_i]$ and the variance (σ^2) is calculated by summing up the values of $[(t_i - t_m)^2 E_i \Delta t_i]$ according to equations (3.2) and (3.3) respectively. The values of normalized variance (σ_θ^2) as given in Table 5.1.2 is obtained as $\frac{\sigma^2}{t_m^2}$ according to the equation (3.6).

Table 5.1.1. Sample calculation of mean and variance

t_i (min)	C_i (g/m^3)	Δt_i (min)	$C_i \Delta t_i$ ($g\text{-}m^{-3}$ min)	E_i $(min)^{-1}$	$t_i E_i \Delta t_i$ (min)	$(t_i-t_m)^2 E_i \Delta t_i$ $(min)^2$
0	0	0	0	0	0	0
9.7	0.05	9.7	0.54	1.4e-4	0.01	1.10
13.7	3.97	4.0	15.8	8.5e-3	0.45	19.9
20.7	12.2	7.0	85.3	2.5e-2	3.79	54.1
25.7	17.1	5.0	102.4	3.5e-2	5.88	27.5
30.7	15.1	5.0	50.2	3.2e-2	3.97	5.57
35.7	8.53	5.0	42.5	1.8e-2	3.27	0.43
39.7	5.95	4.0	27.8	1.4e-2	2.37	0.19
45.7	4.44	6.0	31.1	9.5e-3	3.12	5.21
51.7	3.52	6.0	17.5	7.5e-3	1.95	7.25
55.7	2.77	4.0	13.8	5.9e-3	1.59	10.5
61.7	2.48	6.0	12.4	5.3e-3	1.54	15.2
67.7	2.44	6.0	14.5	5.2e-3	2.14	28.1
77.7	1.55	10.0	15.5	3.5e-3	2.75	55.4
82.7	1.52	5.0	8.11	3.4e-3	1.44	35.1
92.7	1.03	10.0	10.3	2.2e-3	2.05	57.1
100.7	0.32	8.0	2.54	5.8e-4	0.54	21.5
113.7	0.11	13.0	1.31	2.1e-4	0.32	15.2
129.7	0.08	15.0	1.35	1.8e-4	0.38	24.5

$t_m = \Sigma(t_i E_i \Delta t_i)$ $\sigma^2 = \Sigma(t_i-t_m)^2 E_i \Delta t_i$

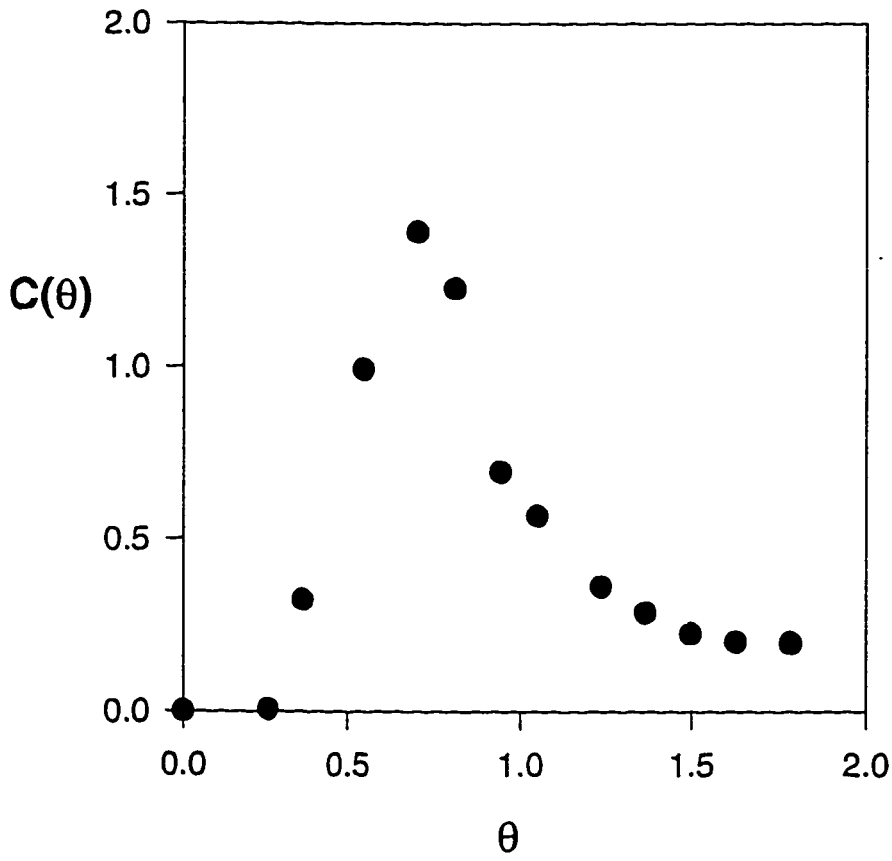

Figure 5.1.1 C curve showing experimental data obtained from pulse tracer input.

Table 5.1.2. Reactor Peclet number from RTD experimental data

σ_θ^2	U_g ($m\ s^{-1}$)	D_L ($m^2\ s^{-1}$)	Pe (Calculated)	Pe (Exptl)
0.27	0.0144	4.9 e-5	185.2	6.03
0.23	0.0138	4.7 e-5	184.4	7.45
0.20	0.0140	4.8 e-5	184.7	9.04
0.23	0.0106	3.7 e-5	179.1	7.63

Data:
$D_{JA} = 7.6\ E\text{-}6\ (m^2\ s^{-1})$
$d_p = 2.0\ E\text{-}3\ (m)$
$\nu = 0.32$

From the literature, Ruthven, D. M. (1984):
$D = \gamma_1 * D_{JA} + \gamma_2 * d_p * U_g/\nu$
$\gamma_1 = 0.45 + 0.55 * \nu$
$\gamma_2 = 0.5$

The reactor Peclet number is then evaluated using equation (3.8) through Newton-Raphson techniques and the results are compared with the correlation obtained from literature, Ruthven, D. M (1984), (see Table 5.1.2). The large difference between the Peclet numbers could be due to the wide size distribution of the particle in the biofilter. The Peclet number obtained through correlation uses a single particle diameter (2 mm) whereas the particles in the biofilter could range from the size of a dust particle to the size of lumps having a diameter greater than 2 mm. The formation of lumps is inevitable due to the presence of moisture in the biofilter bed. This large range of particle size must have increased the mixing in the biofilter. The extent of mixing is also seen from Figure 5.1.1 where the second part of the curve prolongs thereby signifying some dispersion. If the biofilter would have followed a plug flow regime the second part of the curve would have been a mirror image of the first part i.e. the curve would have represented a perfect pulse. But as is seen from the above said figure the second part of the curve lengthens, which suggests that the biofilter exhibits some dispersion and the assumption of plug flow is not good. Another reason that could have enhanced the mixing could be due to the porous nature of the packing. In such cases the molecules of the fluid may enter into the pores apart from passing the particle superficially.

5.2 Biofilter experiments and model validation

Results from steady state biofiltration of toluene vapor are given in Table 5.2.1. This table compares the model-predicted and experimentally-observed removal rates.

Table 5.2.1. Comparison between predicted removal rates and experimentally found removal rates for toluene vapor

τ min	Moisture %	C_{ji} g m^{-3}	C_{je} g m^{-3}	Load g m^{-3} h^{-1}	R_{exp} g m^{-3} h^{-1}	R_{model} g m^{-3} h^{-1}	% Error
2.01	30	2.17	1.02	64.2	33.6	25.4	-24.4
2.01	50	2.17	0.863	64.2	39.0	40.6	+3.98
2.01	70	2.17	0.889	64.2	37.9	38.8	+2.50
1.99	30	3.00	1.87	90.0	33.7	33.3	-1.18
1.97	30	4.02	2.14	122.4	57.1	49.7	-12.9

Removal rate is defined as mass removed per volume of packing material per time. The space time, the inlet and the outlet toluene concentrations, and the load for different sets are also reported. The load is given by C_{ji}/τ and the removal rate is given by $(C_{ji}-C_{je})/\tau$. For model-predicted removal rates, C_{je} is the value predicted at h=H.

The steady state model equations were solved using a computer code developed in the present study. The computer code is based on the method of orthogonal collocation (Appendix A) which reduces the ordinary differential equations to algebraic equations. The resultant equations were solved using DNEQNF subroutine from IMSL package. This subroutine is based on Levenberg-Marquardt algorithm and a finite difference approximation to the Jacobian. The computer code is given in Appendix B. The values of all parameters used in solving steady state axial dispersion model is reported in Table 5.2.2.

The parameters were either determined from independent experiments or estimated from values reported in the literature. The effective biofilm thickness (δ)was found through a trial and error procedure as described by Zarook *et. al.*, (1993). It is the thickness at which 99% of either toluene or oxygen is utilized in the biofilm. Numerical results obtained for effective biofilm ranges from 30μm to 40μm. The value of porosity (ν) was also determined experimentally. Porosity (ν) and biolayer surface area (A_s) were correlated with moisture content (x_{H2O}) as will be described in section 5.3. An average value of the Peclet number (Pe = 7.53) calculated using RTD studies was used in solving the model.

Table 5.2.2. Value of the parameters used in solving the model equations

Parameters	Values	Units	References
A_s	$242\ x_{H2O} - 174\ x^2_{H2O}$	m^{-1}	present study
C_{oi}	275.0 e-3	$kg\ m^{-3}$	1
D_{ow}	2.41 e-9	$m^2\ s^{-1}$	1
D_{jw}	1.03 e-9	$m^2\ s^{-1}$	1
$f(X_v)$	0.195	-	1
K_{fi}	78.94	$g\ m^{-3}$	1
K_O	0.25	$g\ m^{-3}$	1
K_i	11.03	$g\ m^{-3}$	1
m_o	34.4	-	1
m_i	0.27	-	1
Pe	7.53	-	present study
X_v	100.0	$kg\ m^{-3}$	1
Y_{Oi}	0.341	$kg\ kg^{-1}$	1
Y_i	0.708	$kg\ kg^{-1}$	1
ν	$0.44(1-x_{H2O})$	-	present study
δ	30-40	μm	present study
μ_i	1.5	h^{-1}	1

[1] Zarook S. and Baltzis B. C.,1993

The comparison between model predicted concentration and experimental values along the biofilter for five different experimental conditions reported in Table 5.2.1 are given in Figures 5.2.1-5.2.5. Removal rate is calculated based on the inlet and the exit concentrations. But concentration profiles given in these figures show that agreement is also good at intermediate points. Figure 5.2.6 shows the dimensionless concentration of toluene and oxygen in the biolayer at h = 0.5H. Toluene is predicted to be depleted before oxygen in the biolayer. However, at high concentrations of toluene it was observed that oxygen depletes before toluene.

5.3 Moisture contents and its effect on biofilter performance

It is seen from Figures 5.3.1 & 5.3.2 that the removal efficiency, given as (Cji - Cje)/Cji, of the toluene along the column increases when the moisture of the bed was increased to 50%. At 70% moisture content the removal efficiency dropped slightly. This implies that the biofilter works more efficiently in a certain range of moisture content.

Figure 5.3.3 shows the comparison between model predicted versus experimentally found removal rates for various moisture contents. They are in excellent agreement. Of all the moisture experiments the removal rate at 30% was least but increased when the moisture content was increased to 50% but at higher moisture content the removal rate flattened (Figure 5.3.3). This could be explained as the full growth of biolayer surface area must not have been supported by 30% moisture present in the bed. An increase in the moisture content could have provided a more hospitable environment for the microorganisms to grow leading to an increase in the removal rate.

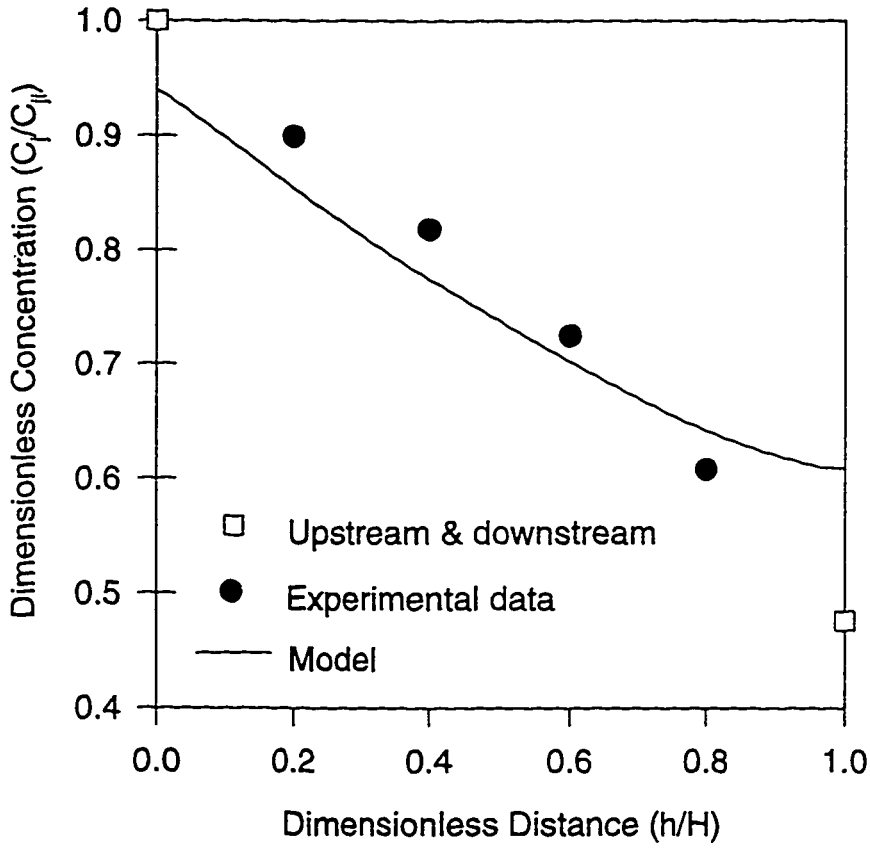

Figure 5.2.1 Model predicted toluene concentration profile and experimental data. $C_{Ti} = 2.17$ g m^{-3}, $\tau = 2.01$ min, $x_{H_2O} = 30\%$, $O_2 = 21\%$.

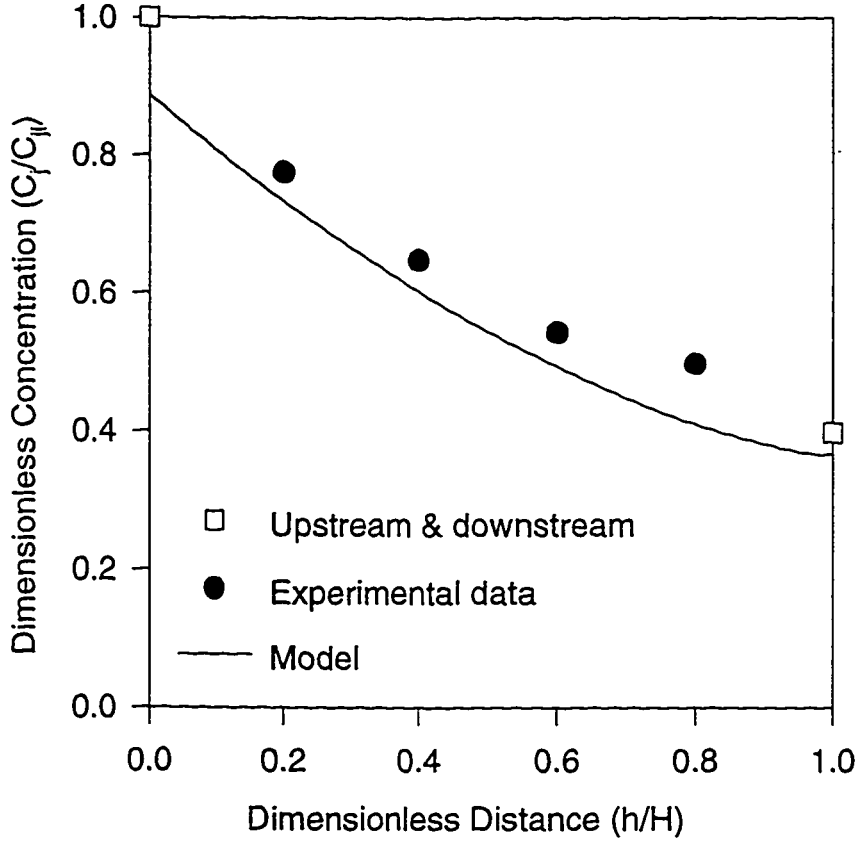

Figure 5.2.2 Model predicted toluene concentration profile and experimental data $C_{Ti} = 2.17$ g m^{-3}, $\tau = 2.01$ min, $x_{H2O} = 50\%$, $O_2 = 21\%$.

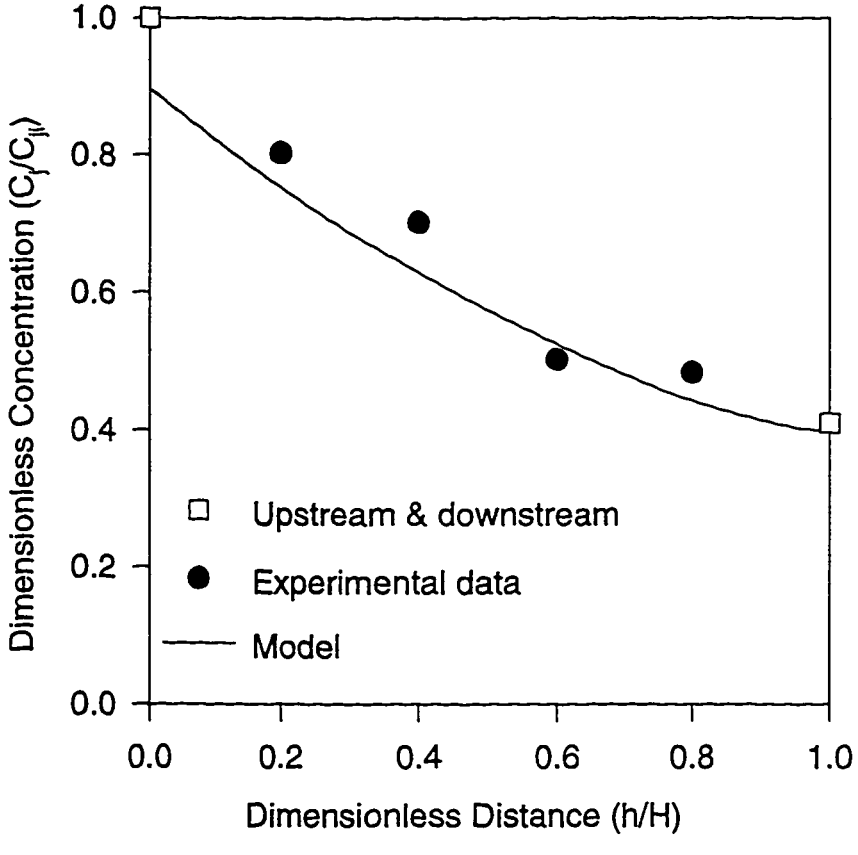

Figure 5.2.3 Model predicted toluene concentration profile and experimental data $C_{Ti} = 2.17$ g m^{-3}, $\tau = 2.01$ min, $x_{H2O} = 70\%$, $O_2 = 21\%$.

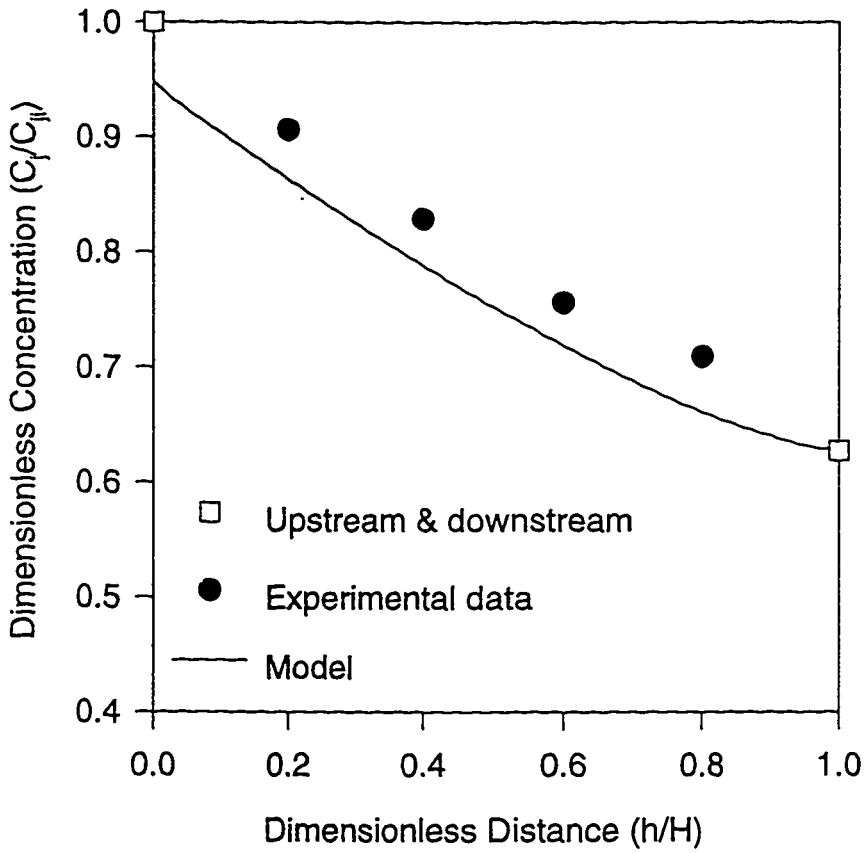

Figure 5.2.4 Model predicted toluene concentration profile and experimental data. $C_{Ti} = 3.0$ g m^{-3}, $\tau = 1.99$ min, $x_{H2O} = 30\%$, $O_2 = 21\%$.

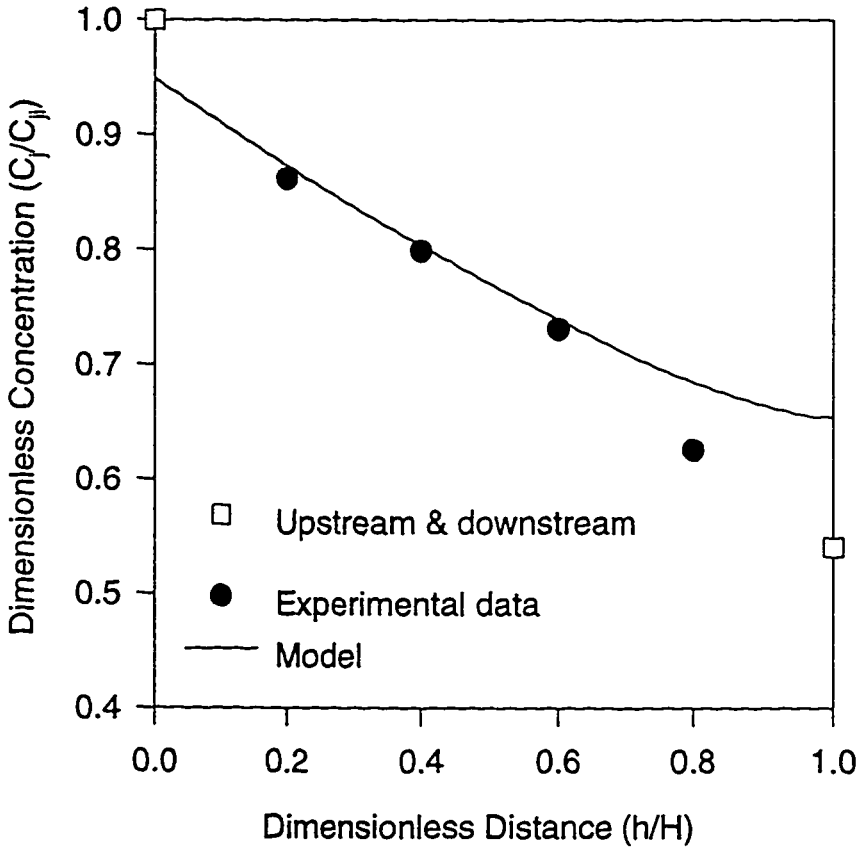

Figure 5.2.5 Model predicted toluene concentration profile and experimental data. $C_{Ti} = 4.02$ g m^{-3}, $\tau = 1.97$ min, $x_{H2O} = 30\%$, $O_2 = 21\%$.

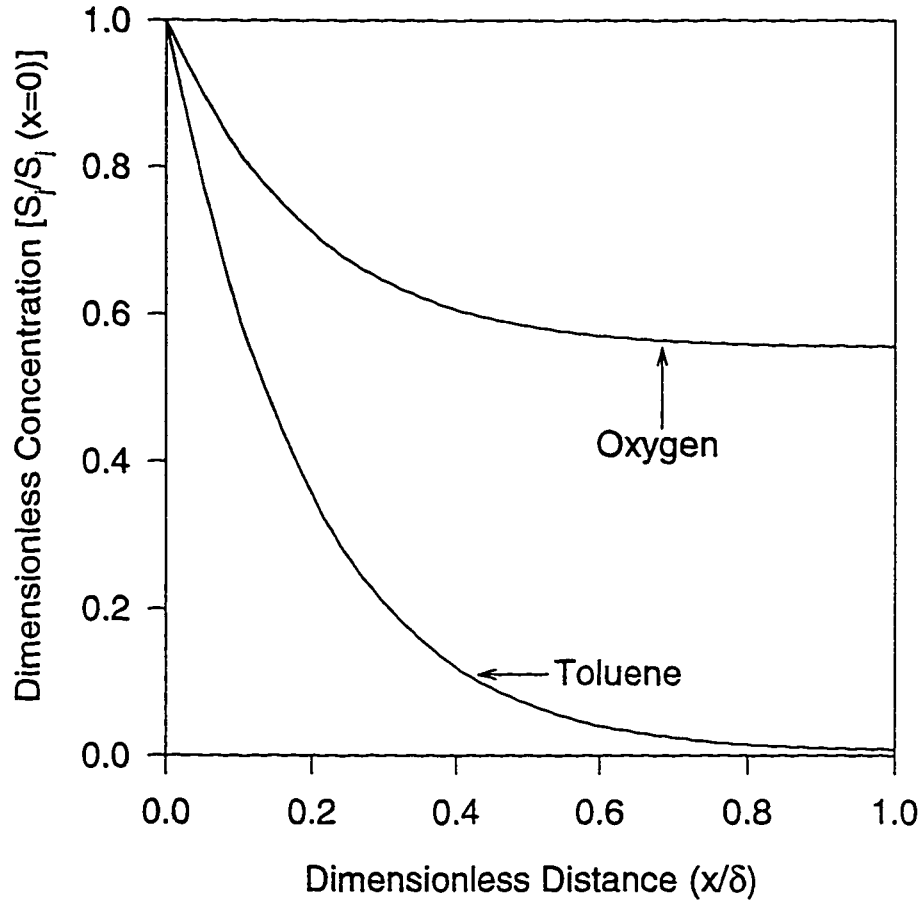

Figure 5.2.6 Concentration profile in the biofilm at h = 0.5 H.

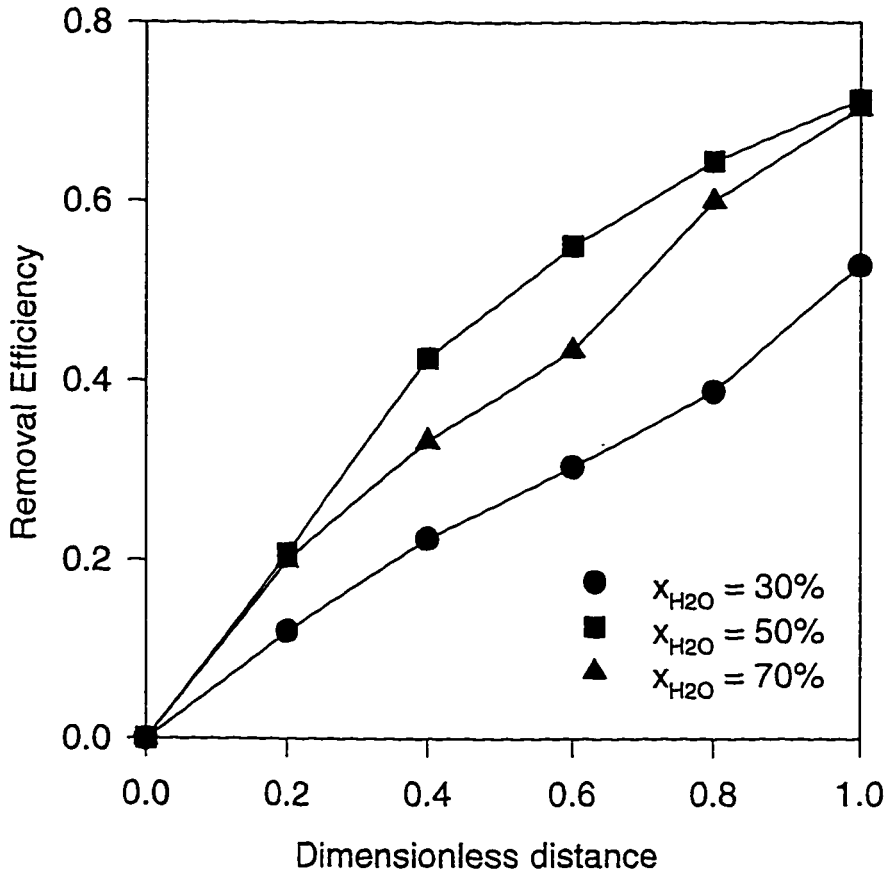

Figure 5.3.1. Experimental data obtained for different moisture conents when C_{Ti} = 1.5 g m^{-3}, τ = 2.03 min and O_2 = 21%.

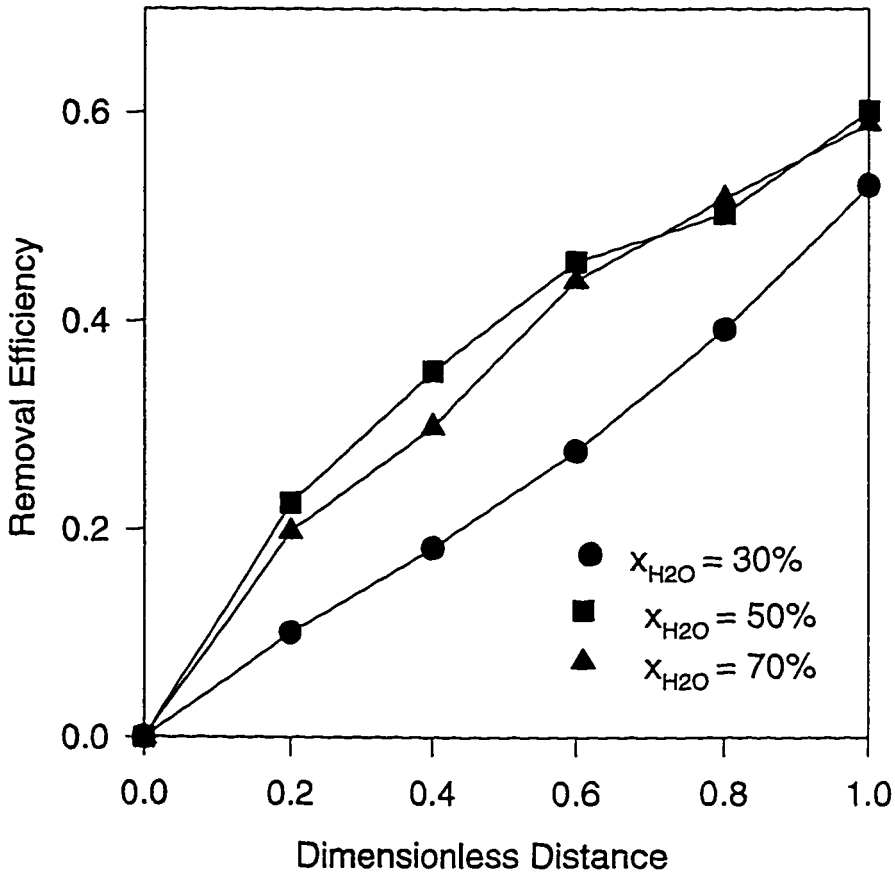

Figure 5.3.2 Experimental data obtained for different moisture contents when $C_{Ti} = 2.17$ g m^{-3}, $\tau = 2.01$ min and $O_2 = 21\%$.

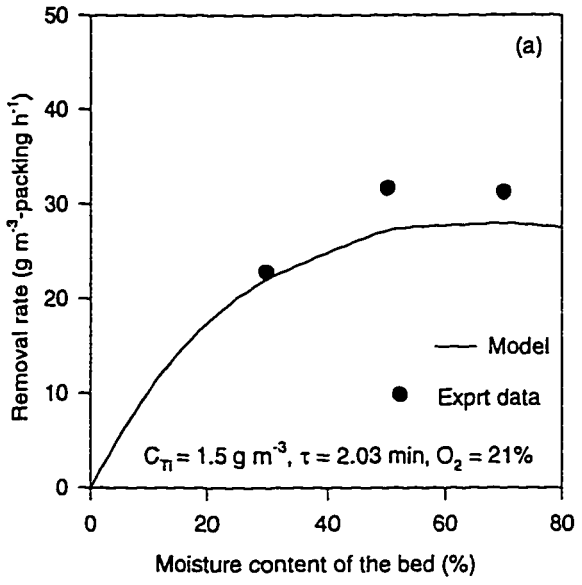

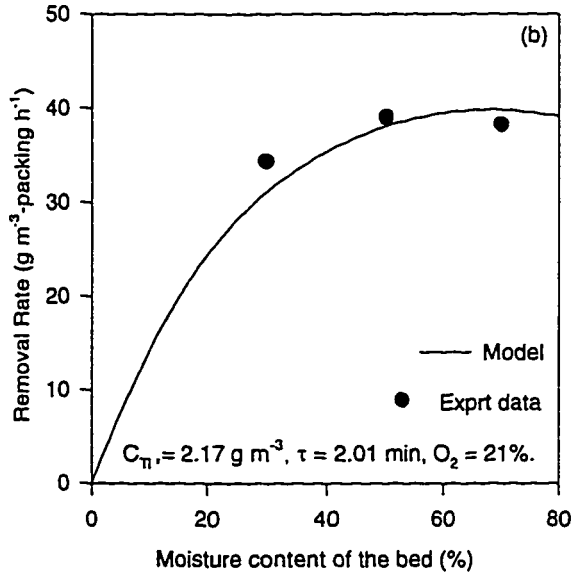

Figure 5.3.3. Comparison between the model predicted removal rates and experimentally obtained removal rates for various moisture contents.

This is observed at 50% moisture content of the bed. At higher moisture content (70%) flooding was observed at the bottom of the biofilter. This could have happened due to the percolation of water from the top. This resulted not only in an increase in the pressure drop but also a slight reduction in the removal rate. The decline in the removal rate can have several reasons. The water percolating down could have taken alongwith it some nutrients and microbes and there could be formation of channels. Table 5.3.1 shows the increase in the removal rates at different moisture content when compared to 30% moisture condition. The value of the porosity of the bed at different moisture contents is reported in Table 5.3.2. The porosity at various moisture content was also determined experimentally as follows. To a known volume of dry packing material water was added until it gets saturated. This procedure was repeated number of times and the average value of the volume of water added was determined. The moisture content (x_{H2O}) was then estimated as the average value of the volume of water divided by the volume of the packing material. A correlation between porosity (ν) and moisture content (x_{H2O}) obtained as $\nu = 0.44(1-x_{H2O})$ was used in the solution of the model. The external surface area of particles which is covered by biofilm (A_s) is estimated by the procedure described by Zarook *et. al.* (1993). The procedure involves fitting the value of A_s for some experimental data sets and subsequently using this value in predicting the concentrations under conditions which were not used in the fitting approach. Figures 5.3.4 - 5.3.6 show the comparison between model, fitted (a) or predicted (b), profiles and experimental data points obtained at different moisture levels. Data reported in Figures 5.3.4a, 5.3.5a, and 5.3.6a are used to find A_s.

Table 5.3.1 Experimental results obtained at different moisture content of the biofilter

Moisture (%)	Inlet conc. (gm^{-3})	Exit conc. (gm^{-3})	Space time (min)	Removal; efficiency (Expt)	Removal rate (Expt) $gm^{-3}h^{-1}$	Increase in removal rate compared to 30% moisture
30	1.50	0.727	2.03	51.5	22.8	
50	1.50	0.430	2.03	71.3	31.6	+38.6
70	1.50	0.444	2.03	70.4	31.3	+37.2
30	2.17	1.019	2.01	52.5	34.0	
50	2.17	0.863	2.01	60.2	39.0	+14.6
70	2.17	0.889	2.01	58.5	37.9	+11.5

Table 5.3.2 Experimentally obtained porosity at different moisture contents

Moisture	Porosity
0.3	0.32
0.4	0.25
0.5	0.20
0.6	0.12

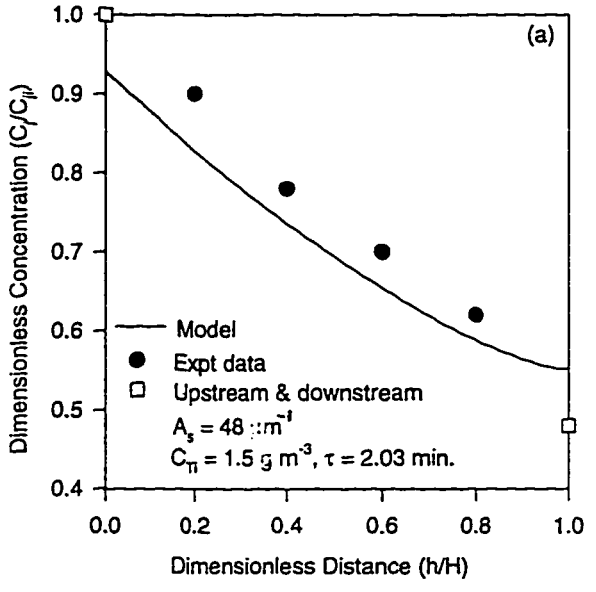

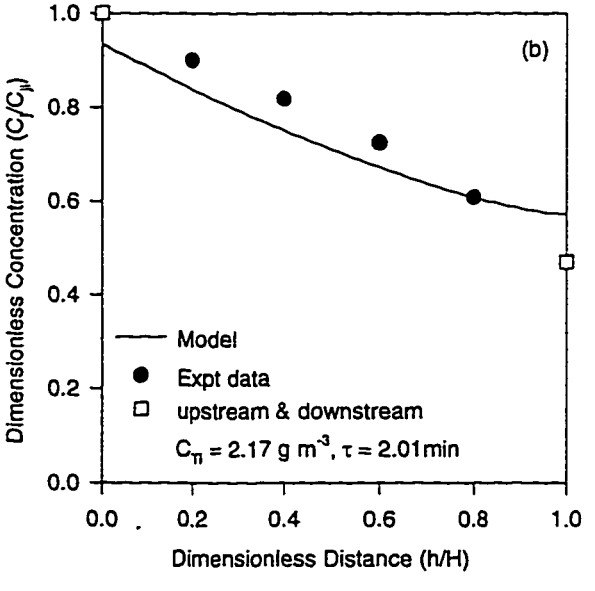

Figure 5.3.4. Comparison between concentration profile generated by model and experimental data. x_{H2O} = 30%, O_2 = 21%.

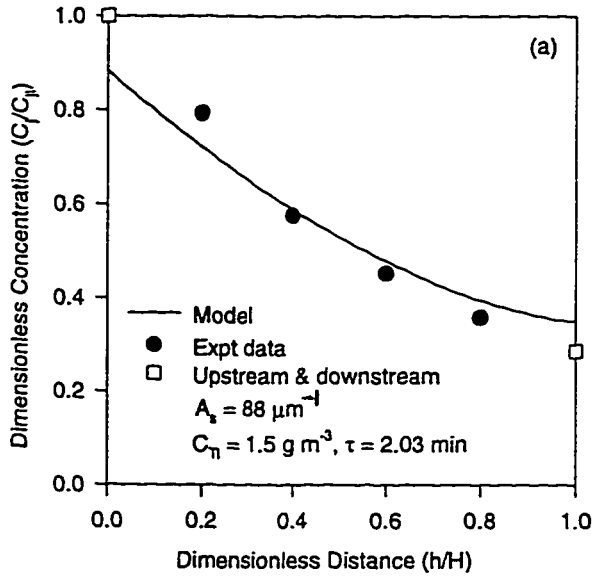

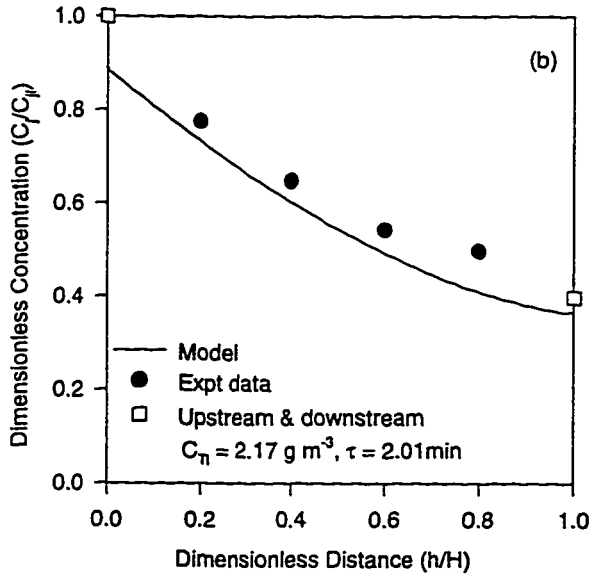

Figure 5.3.5. Comparison between concentration profile generated by model and experimental data. x_{H2O} = 50%, O_2 = 21%.

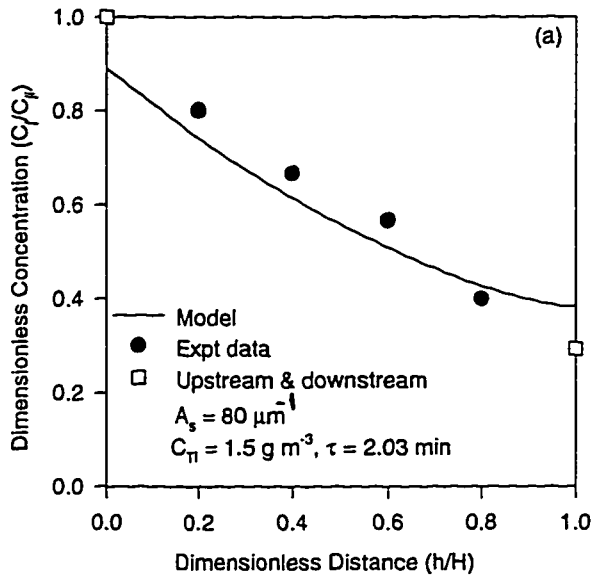

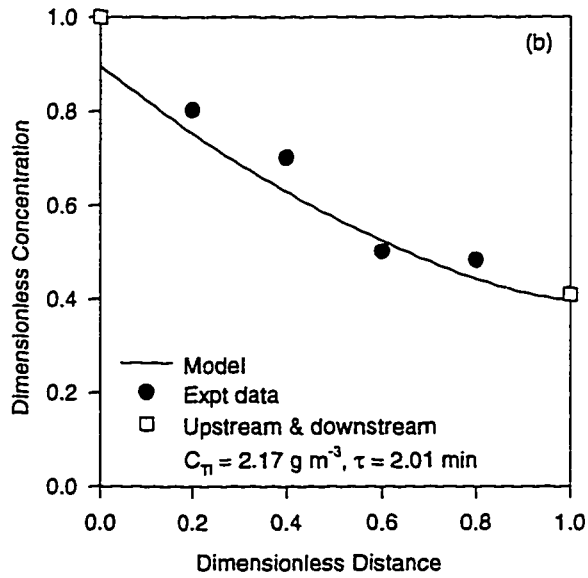

Figure 5.3.6 Comparison between concentrationprofile generated by model and experimental data. x_{H2O} = 70%, O_2 = 21%.

The respective values of A_s had been used to generate the model-predicted concentration profiles for second experimental data sets which are shown in Figures 5.3.4b, 5.3.5b, and 5.3.6b. A correlation between biolayer surface area (A_s) and moisture content was also obtained and subsequently used in the solution of the model. $As = 242\ x_{H2O} - 174\ x^2_{H2O}$. Figure 5.3.7 shows the fitted correlation of the biolayer surface area with the experimental found values. It is seen from the figure that after a certain range of moisture content the biolayer surface area decreases. This could be attributed to the fact that at high water content in the biofilter the microflora does not get enough particle surface area for immobilization, thereby decreasing the biolayer surface area.

5.4 Effect of oxygen

The oxygen experiment was started with low concentrations of toluene vapor. The removal efficiency of the biofilter is shown in Figures 5.4.1 - 5.4.3 for different inlet concentration of toluene and at various oxygen concentrations. As is evident from the figure that increasing the oxygen concentration improves the removal efficiency of the biofilter. Results obtained from this experiment has also been tabulated in Table 5.4.1. The magnitude of difference is small in the first case ($C_{Ti} = 1.5\ g\ m^{-3}$) where the inlet concentration of toluene is low. This is because toluene is an easily biodegradable compound and increasing the oxygen concentrations at low concentration of toluene will have no major change. The effect of oxygen on a compound which is not easily bidegradable could be prominent even at low inlet concentrations. As predicted by the model (Figure 5.2.6) at low concentrations of toluene, oxygen is in excess but at high

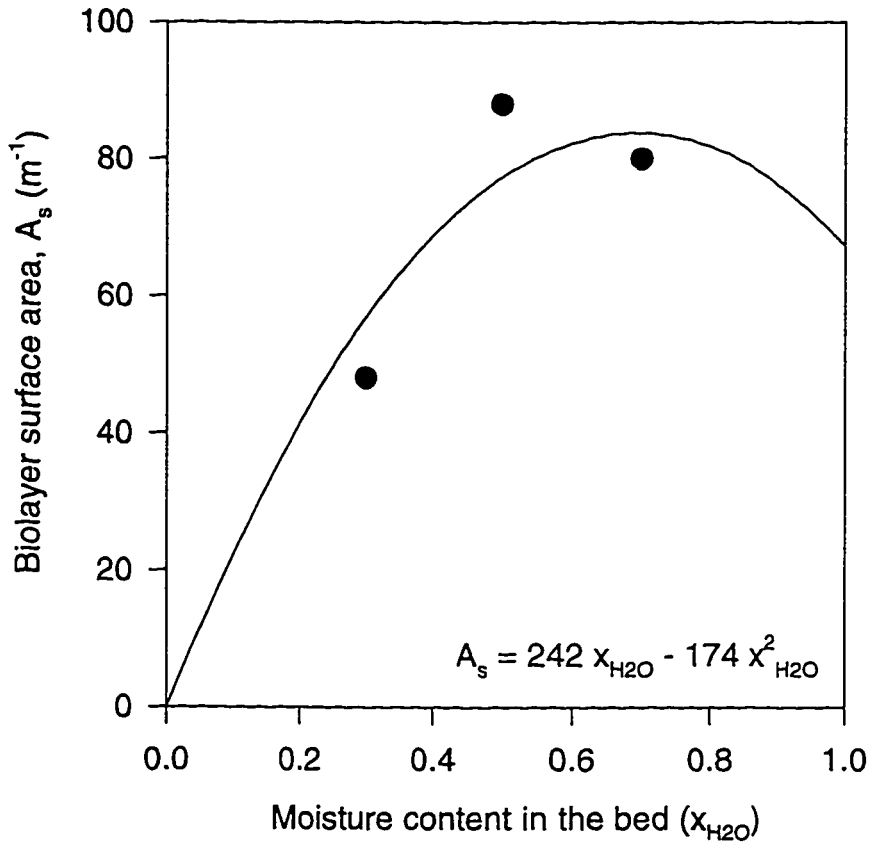

Figure 5.3.7. Variation of biolayer surface area with respect to moisture content of the bed

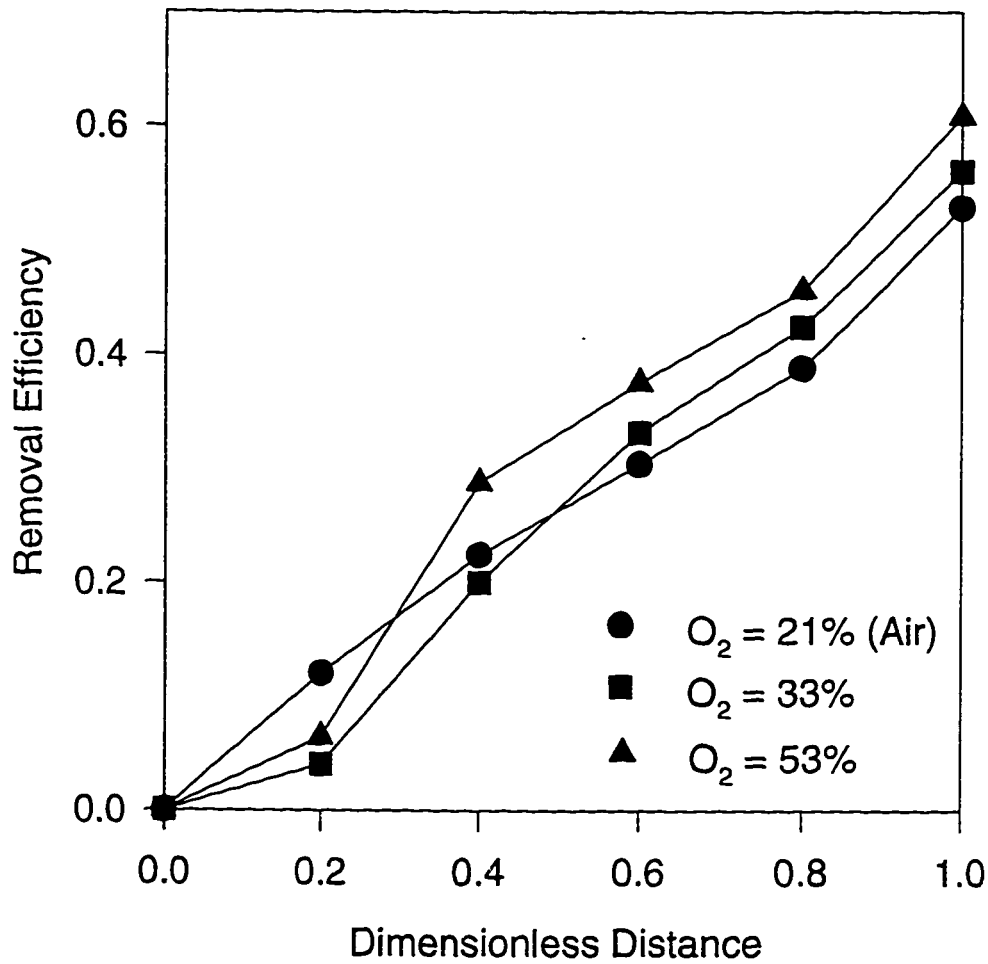

Figure 5.4.1. Experimentally obtained results at different inlet concentrations of toluene and different percentages of oxygen. $C_{Ti} = 1.5\ gm^{-3}$, $\tau = 2.03$ min, $x_{H2O} = 30\%$.

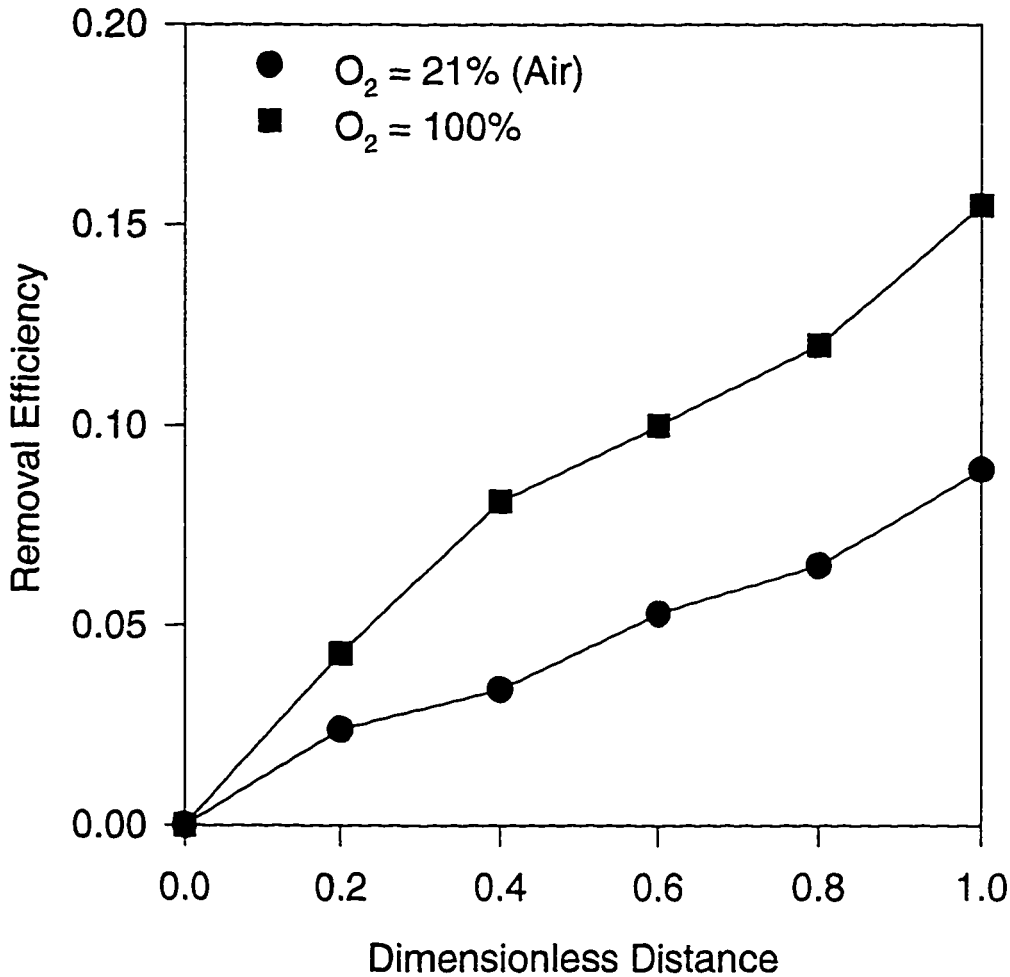

Figure 5.4.2. Experimentally obtained results at different inlet concentrations of toluene and different percentages of oxygen. $C_{Ti} = 10\ gm^{-3}$, $\tau = 0.976$ min, $x_{H2O} = 30\%$.

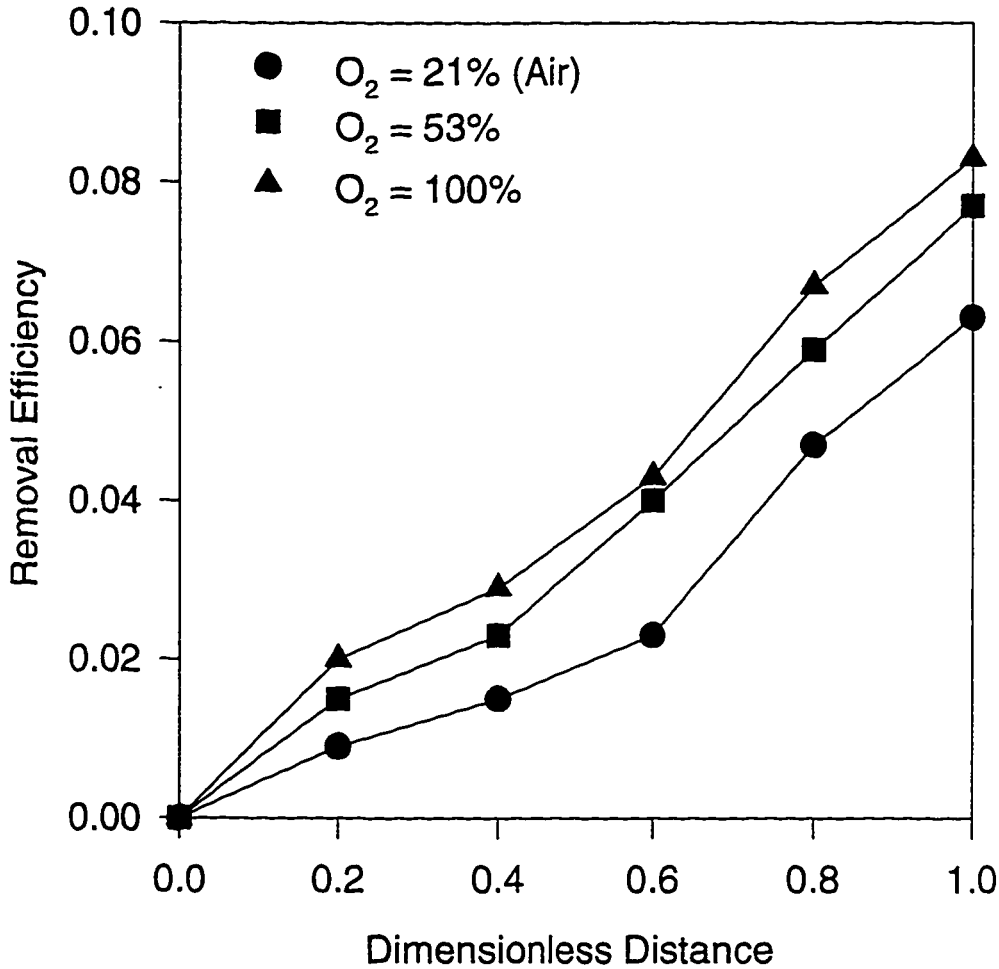

Figure 5.4.3. Experimentally obtained results at different inlet concentrations of toluene and different percentages of oxygen. C_{Ti} = 17.5 gm^{-3}, τ = 0.785 min, x_{H2O} = 30%.

Table 5.4.1 Experimental results for different concentrations of oxygen

O_2 (fraction)	Inlet conc. ($g\ m^{-3}$)	Exit conc. ($g\ m^{-3}$)	Space time (min)	Removal efficiency	R_{exp}	Removal percentage compared to air
0.21 (air)	1.5	0.727	2.03	51.5	22.8	
0.33	1.5	0.660	2.03	56.0	24.8	+8.77
0.53	1.5	0.57	2.03	62.0	27.4	+20.2
0.21 (air)	10.0	9.11	0.975	8.9	54.7	
1.0	10.0	8.43	0.975	15.7	96.5	+76.4
0.21 (air)	17.5	16.44	0.785	6.06	84.3	
0.53	17.5	16.19	0.785	7.48	103.0	+22.1
1.0	17.5	16.09	0.785	8.05	111.2	+31.9

concentrations of toluene, oxygen becomes the limiting reactant. Supply of oxygen could improve the degradation when inlet concentrations of toluene is high. This is supported with the experimental results shown in Figure 5.4.2a. One can see more clearly from Table 5.4.1. The second set of data in Table 5.4.1, at toluene concentration of 10g m^{-3} shows the increase in the removal rate by 76.4% when the concentration of oxygen is increased to 100%. The next set of data however, does not show much difference where the inlet concentration of toluene is increased to 17.5gm^{-3}. This could probably be due to high substrate inhibition at high concentration of toluene.

The model was also used to predict the concentartion profile for different oxygen percentages at high inlet concentrations of toluene. The comparison between model predictions and experiment data shown in Figures 5.4.4 - 5.4.6 are good for most of the cases but at high toluene concentrations the model under predicts especially when inlet toluene concentration equals to 17.5 g m^{-3}. As explained earlier the reason for lower experimental values could be due to the inhibition nature of the substrate. It can be seen from Figure 5.4.5 (c) and (d) that although, oxygen concentrations (both experimental and model predictions) seem to be constant along the column, numerical results show that, inside the biofilm, oxygen concentrations profile are different.

5.5. Pressure drop in the biofilter

The measured pressure drop in the biofilter has been compared with the pressure drop calculated through Ergun equation given in Table 5.5.1. Since the packing material was sieved with 2mm mesh hence, the particle diameter of 2mm was chosen

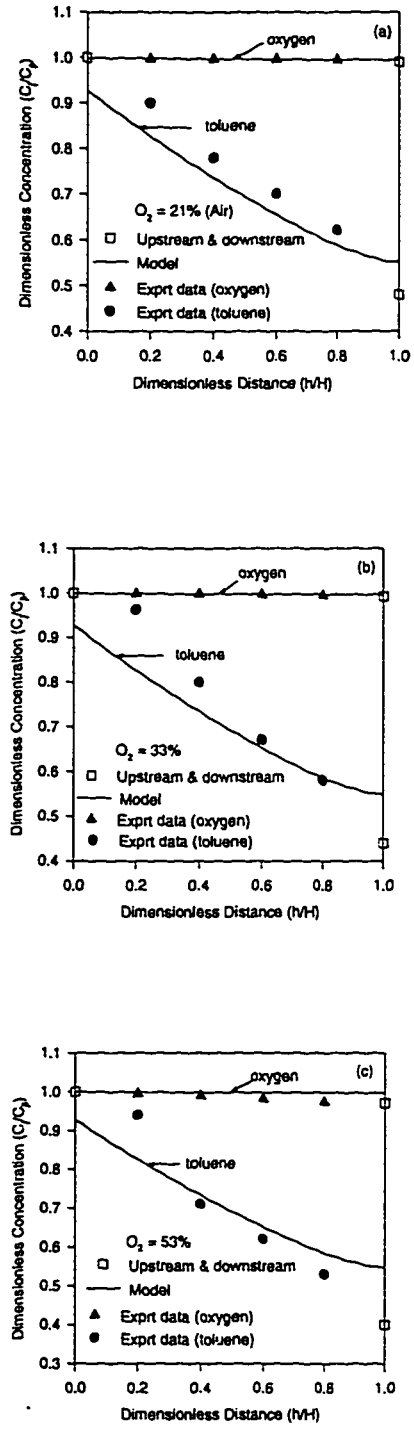

Figure 5.4.4. Comparison between model-predicted toluene concentration profile and experimental data. The operating conditions are C_{Ti} = 1.5 g m^{-3}, τ = 2.03 min, x_{H2O} = 30%.

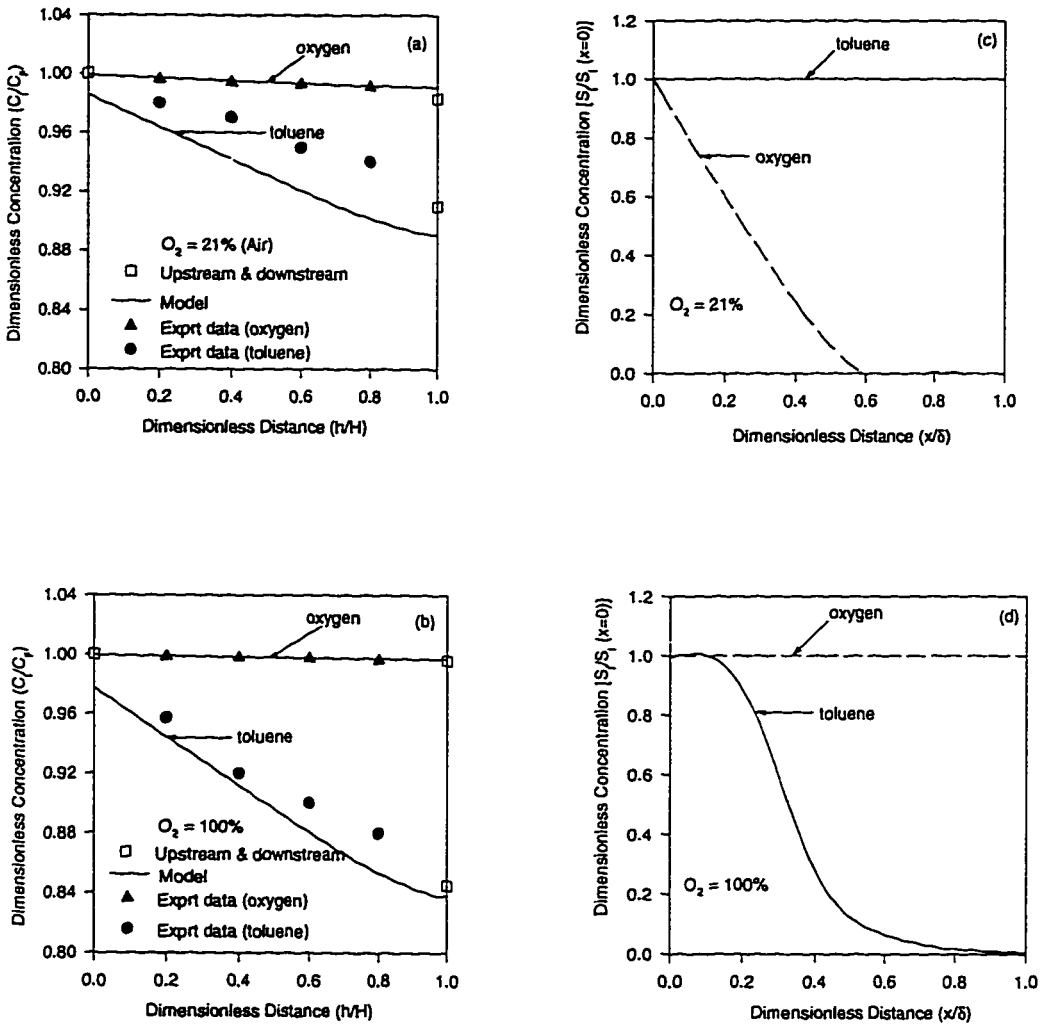

Figure 5.4.5. Comparison between model predicted toluene concentration profile and experimental data. The operating conditions are C_{Ti} = 10 g m^{-3}, τ = 0.975 min, x_{H2O} = 30%. (c) and (d) are profiles in the biofilm.

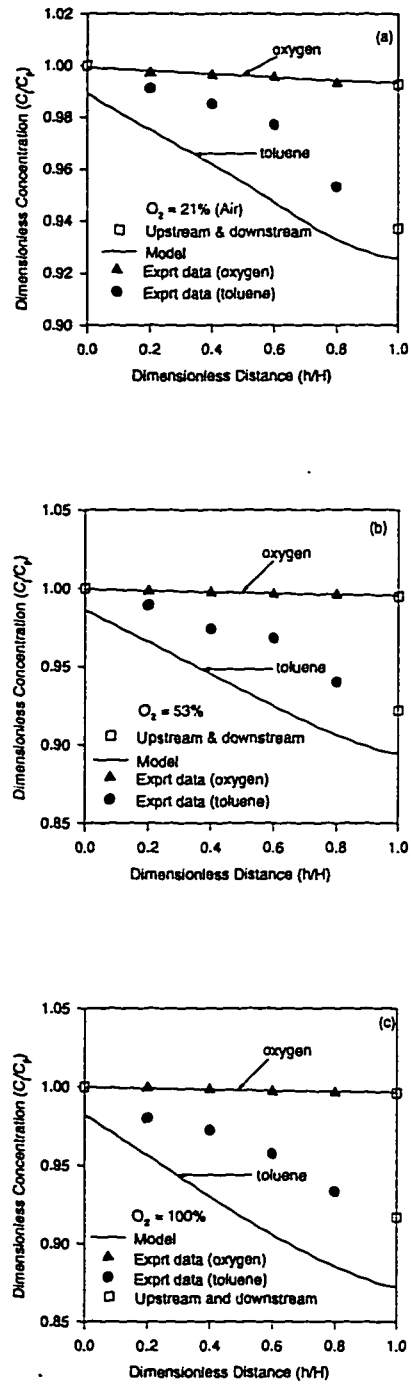

Figure 5.4.6. Comparison between the model-predicted toluene concentration profile and experimental data. The operating conditions are C_{ti} = 17.5 g m^{-3}, τ = 0.785 min, x_{H2O} = 30%.

Table 5.5.1 Comparison between experimentally obtained pressure drop and calculated values through Ergun equation.

Moisture (%)	Porosity (ν)	d_p (mm)	Re_p	f_p	$\Delta P/L$ (Expt) cm H_2O/m-bed	$\Delta P/L$ (Ergun eq) cm H_2O/m-bed
0.3	0.32	2	1.015	149.5	3.28	0.52
0.5	0.20	2	0.862	175.5	4.22	2.95
0.7	0.12	2	0.784	192.9	9.37	16.5

Ergun equation

$\Delta P/L = [fp\ \rho\ U_g^2\ (1-\nu)]/[d_p\ \nu^3]$

$fp = 150/Re_p + 1.75$

$Re_p = [d_p\ \rho\ U_g]/[(1-\nu)\ \mu_r]$

$\rho = 1.17$ kg m^{-3}

$U_g = 5.31$ e-3 m s^{-1}

$\mu_r = 1.8$ e-5 kg m^{-1} s^{-1}

for the calculation of pressure drop through Ergun equation. However, the particle size could range from the size of a dust particle to the size of lumps which could be greater than 2mm. According to Ottengraf and van den Oever (1983), Ergun equation, which is used to estimate pressure drops in packed bed, could also be used for the case of biofilter as well, but the experimentally obtained pressure drops are different compared to the calculated values. The reason for this difference as mentioned above could be due to the wide distribution of particle size and due to the presence of high content of moisture which would have contributed to the formation of lumps. At lower moisture content the formation of large lumps would not have been possible and the particle diameter could have been smaller than 2mm. But,at high moisture contents due to the formation of lumps the particle size could be more than 2mm, and pressure drop through Ergun equation based on higher particle diameter will be close to experimental value. The difference between the experimental and the calculated pressure drops could also be attributed to the uneven growth of the biofilm around the solid particles.

Experimentally obtained pressure drops are also plotted against moisture contents in Figure 5.5.1. Pressure drop increases with the moisture content of the bed. Although, increase in the moisture content may lead to higher removal rates, higher pressure drop will increase the cost of the operation. Thus, there is an optimum value of moisture content for better performance of the biofilter.

5.6. Sensitivity analysis

The sensitivity of the model was investigated by varying the values of different parameters. Some of the results of the model sensitive parameters are reported here.

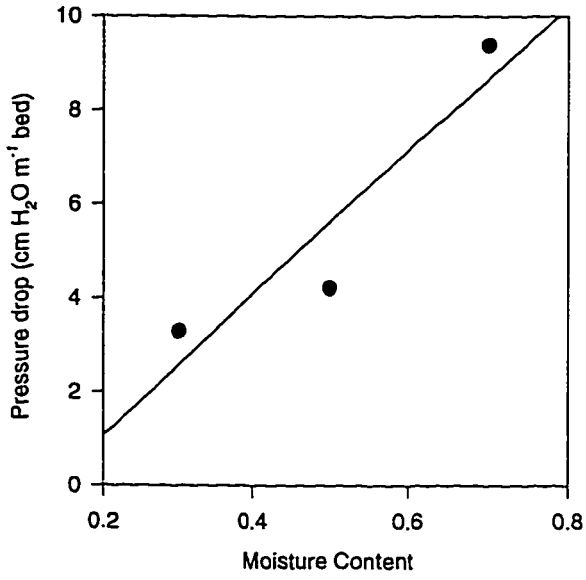

Figure 5.5.1 Variation of pressure drops with moisture content of the bed

Figures 5.6.1 and 5.6.2 show the affect on the removal rate with the change in the values of the parameters. The *x*-axis of the graph represents the assumed relative value of the parameters under study. The *y*-axis of the graphs represents the relative value of the removal rate which is calculated as the predicted removal rate under the assumed value of the parameter divided by the experimentally obtained removal rate for that set of experimental conditions which was taken as basis. Figure 5.6.1 shows the importance of the biolayer surface area (A_s) and the kinetic parameter, μ^*. The non-linear variation of the removal rate with respect to the change in μ^* implies that a zero-order or first-order assumption in the kinetics is very poor and should not be made. The most sensitive of all the parameters is the biolayer surface area (A_s). The method of estimating the value of A_s through fitting has been explained earlier. The graph indicates that if the value of A_s used is smaller than the fitted value, then the error in predicting the removal rate could be quite significant. However, if the value is larger than the fitted value then the error in predicting the removal rate would not be very significant. Figure 5.6.2 shows the sensitivity of the model to the values of the other kinetic parameters and biofilm density (X_v). Of the kinetic parameters shown K_j is very sensitive. It is also seen from the graph that the predicted removal rate is not sensitive to K_{oj}. Figure 5.6.3 shows the concentration profile along the column at different Peclet numbers. The concentration profile at the average value of experimentally obtained Peclet number (Pe = 7.53) shows significant dispersion. This has also been explained in detail in section 5.1.

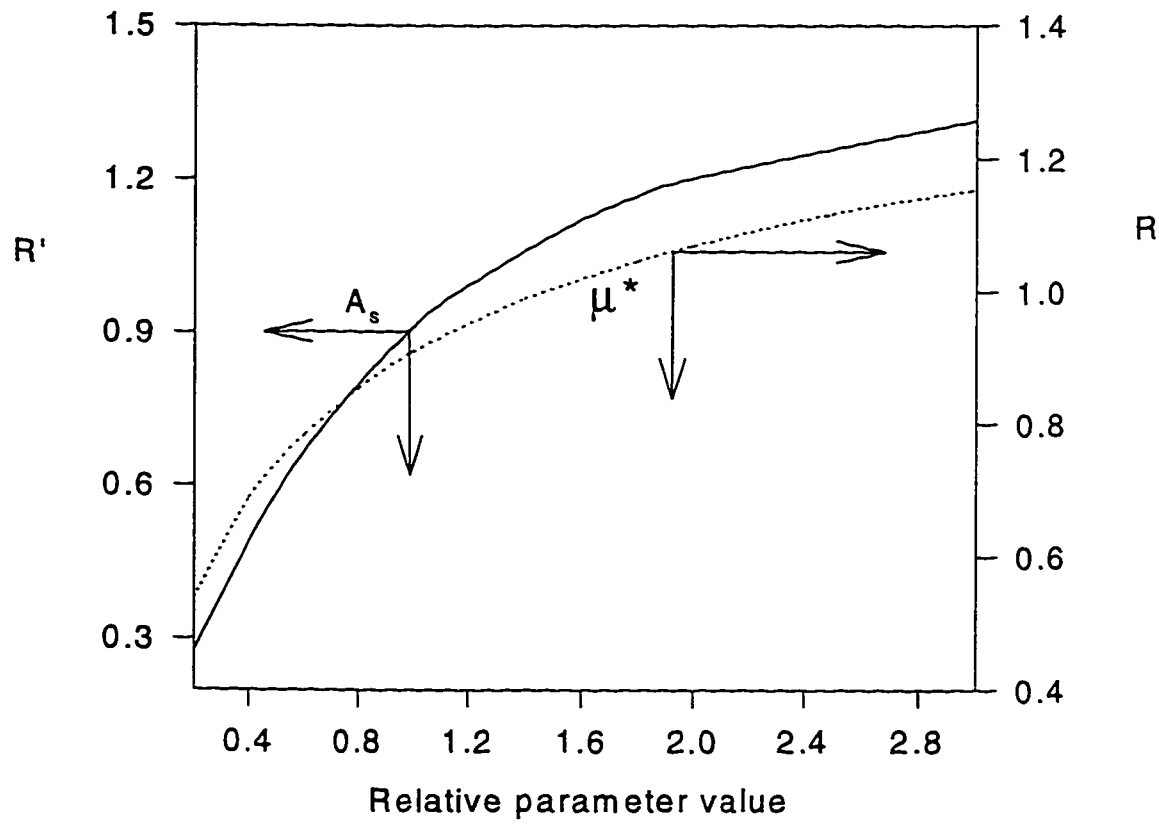

Figure 5.6.1. Sensitivity of the model to the parameters A_s and μ^*. The reference value of the removal rate is 31.5 g m^{-3}-packing h^{-1} when C_{ti} = 1.5 g m^{-3} and τ = 2.03 min. The value for these parameters are given in Table 5.2.2.

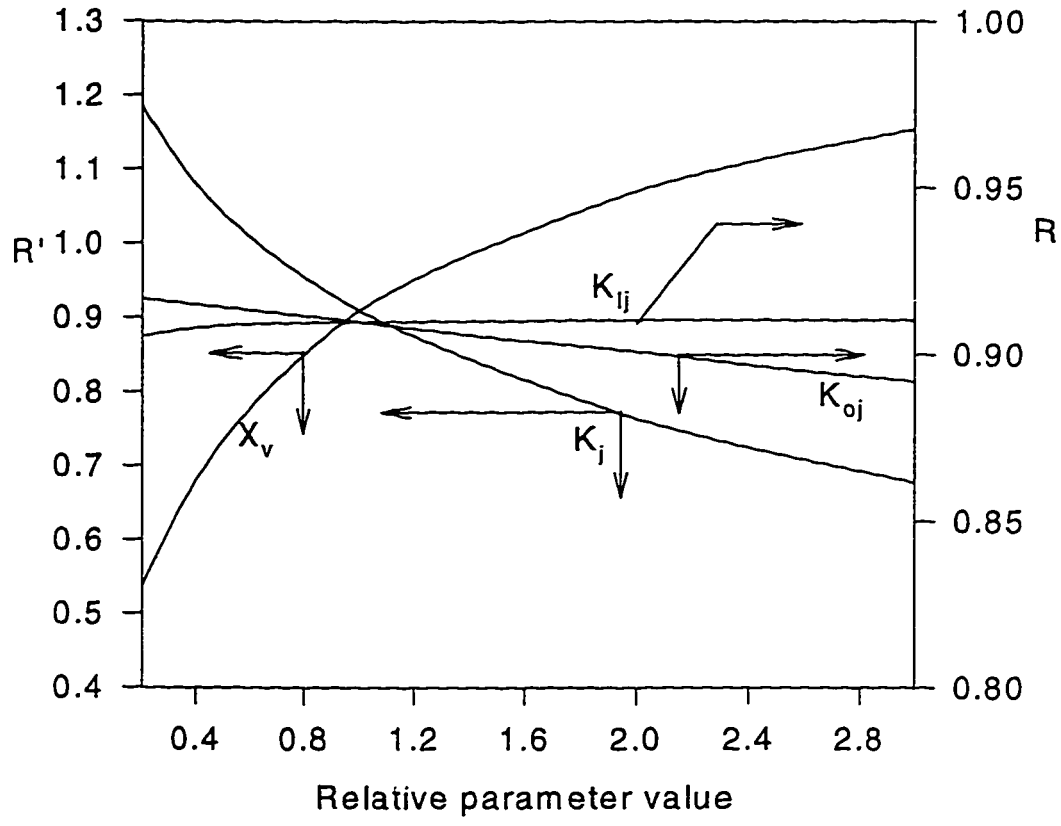

Figure 5.6.2. Sensitivity of the model with respect to the kinetic parameters. The reference value for the removal rate is same as Figure 5.6.1. The reference values for the parameters are given in Table 5.2.2

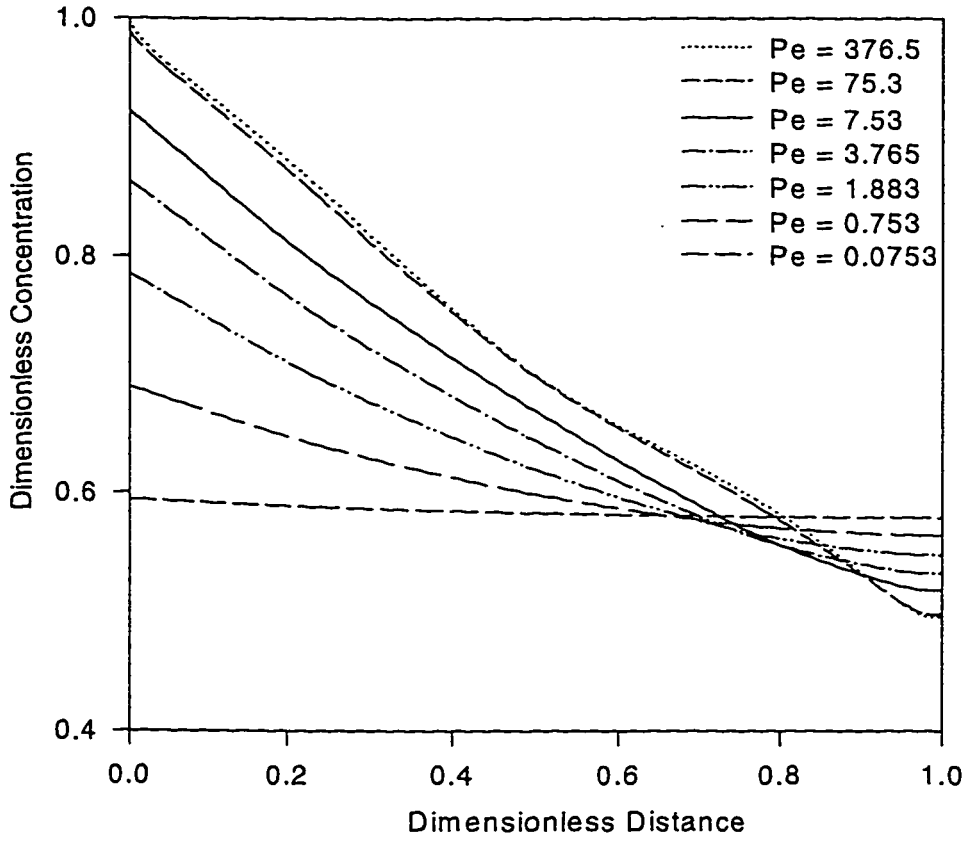

Figure 5.6.3. Sensitivity of the model with respect to the Peclet number. The average value of the experimentally obtained Peclet numbers is 7.53.

Thus, the sensitivity studies show that simple kinetics of zero or first-order assumptions are not very good. At least kinetics in this case is determined by two constants, μ^* and K_j. Furthermore, estimation of biolayer surface area, A_s, should be carried out with care as this parameter is highly sensitive to the removal of toluene. As discussed in section 5.1 the axial dispersion effects should be taken into consideration in theoretical models.

Chapter 6

Conclusions & Recommendations

7.1 Conclusions

The mixing characteristics of a fluid in a biofilter was studied under abiotic conditions. The values of Peclet number (6.0 - 9.0) obtained in this study, indicates that the biofilter works with a significant amount of dispersion. Thus, the assumptions of plug flow used in previous studies (Ottengraf and van den Oever, 1983; Zarook *et. al.*, 1993) is not a good one, and dispersion effects should be considered in developing theoretical biofilter models. Biofiltration of toluene vapor was studied in detail. If operating conditions are perfectly controlled and given enough residence time, 100% removal can be achieved. A steady state biofilter model which incorporates axial dispersion effect has been developed. Along with other parameters, the Peclet number calculated through RTD studies has been used in solving the model. The comparison between experimental data and model predicted concentrations are in good agreement.

moisture contents of the bed. It was observed that the bed performed most efficiently when the moisture content was around 50%. At 30% moisture content in the bed the packing material could not have been able to provide the required water content for the full growth of microbes. At 70% flooding had occurred in the bed. Due to the high moisture load, water could have percolated down creating channels as well as carrying along with it some nutrients and bacteria. Correlations have been obtained regarding the variation of biolayer surface area with the moisture content as well as the variation of bed porosity with the moisture content.

Experiments were also carried out to study the effect of oxygen concentration on the removal of the toluene vapor. It was observed that increase in the oxygen concentration does increases the removal of the pollutant although the difference is not significant at low inlet concentration of toluene vapor. At high inlet concentrations the effect of oxygen was significant. Thus, by enriching the feed with oxygen, desired removal rate could be achieved in a relatively small size biofilter.

The pressure drop in the biofilter is different compared to the calculated values through Ergun equation. This is attributed to the growth of the biofilm around the solid particle and the nature of the packing material. Sensitivity analysis of the model to the values of various parameters showed that biolayer surface area, biofilm density and some of the kinetic parameters are highly important and assumption of simple kinetics is not a good one.

7.2 Recommendations

- The residence time distribution study could be extended for the case when bacteria are present in the biofilter.
- The present correlation for the biolayer surface area can be checked for different packing materials.
- The existing models and biofilter performance could be explored for the non-isothermal case.
- Since biofilter is a non-linear system possibilty of multiple steady states can also be explored.

References

Andrews, J. F., 1968, A mathematical model for the continuous culture of microorganisms utilizing inhibitory substrates. *Biotechnol. Bioenng.* 10, p 707.

Barnes, J. M., Apel, W. A. and Barett, K. B., 1995, Removal of nitrogen oxides from gas streams using biofiltration, *J. of Hazardous Materials*, vol 41, p315.

Bohn, H., 1992, Consider biofiltration for decontaminating gases. *Chemical Engng. Prog.* April, p 34.

Bohn, H., 1993, Biofiltration: Design principles and pitfalls, in Proceedings of the 86h A&WMA meeting, Paper No. 93-TP-52A.01, Air & Waste Management Association, Denver, CO.

Couillard, D., 1994, The use of peat in waste water treatment, *Water Research*, vol 28, no 6, p 1261.

Danckwert P. V., 1953, Continuous flow systems, distribution of residence time, *Chemical Engineering Science*, 2, pp 1-18.

Deshusses, M. A. and Dunn I. J., 1993, Modeling experiments on the kinetics of mixed-solvent removal from waste gas in biofilter, in Proceedings of the 6th European Congress on Biotechnology, Florence.

Deshusses, M. A. and Hamer, G., 1993, The removal of volatile ketone mixtures from air in biofilters, *Bioprocess Eng.* vol 9, p 141.

Dharmavaram, S., 1991, Biofiltration a lean emissions abatement technology, in Proceedings of the 84th A&WMA meeting, Paper No. 91-103.2, Air & Waste Management Association, Vancouver, British Columbia.

Diks, R. M. M., 1992, The removal of dichloromethane from waste gases in a biological trickiling filter, PhD. Thesis, The Eindhoven University of Technology, The Netherlands.

Diks, R.. M. M. and Ottengraf , S. P. P., 1991, Verification studies of a simplified model for removal of dichloromethane from wastes gases using a biological trickling filter, Part1. *Bioprocess Engng* 6, p 93.

Don, J. A., 1985, The rapid development of biofiltration for the purification of diversified waste gas streams. in VDI Berichte 561, VDI Verlag, Dusseldorf, p 63.

Donald, E. S. and Dauglis A. J., 1988, Review of liquid mixing in packed bed biological reactors, *Biotehnol Progress* 4, 3, p 134.

Ergas, S.J., Schroeder, E.D. and Chang, D. P. Y., 1993, in Proceedings of the 86th A& WMA meeting, Paper No. 93-WA-52B, Air & Waste Management Association, Denver, CO.

Fan, L. S., Leyva-Ramos, R., Wisecarver, K. D. and Zehner, B. J., 1990, Diffuson of phenol through a biofilm grown on activated carbon particles in a draft-tube three-phase fluidized-bed bioreactor. *Biotechnol. Bioengng* 41, p 947.

Hodge, D. S. and Devinny, J. S., 1994, Biofilter treatment of ethanol vapors, *Environmmental Progress*, vol 13, no 3, August, p 167.

Hodge, D. S., Medina, V. F., Islander, R. l., and Devinny, J. S., 1991, Treatment of hydrocarbon fuel vapors in biofilters. *Environmental Technol.*,vol 12, p 655.

IMSL Math library user's manual, IMSL Incorporation, USA, 1987.

Leson, G. and Winer A. M., 1991, Biofiltration: An innovative air pollution control technology for VOC emissions. *J. Air Waste Manage. Assoc.* 41, p 1045.

McInnes, R., Jelinek, S., and Putsche, V., 1990, Cuting toxic organics. *Chemical Engng,* Sept., p 108.

Monod, J., 1942, *Recherches sur la Croissance des Cultures Bacterriennes.* Hermann et Cie, Paris.

Oh, Y. S., 1993, Biofiltration of solvent vapors from air. Ph.D. thesis, Rutgers University, New Brunswick, NJ.

Ottengraf , S. P. P., 1986, Exhaust gas purification, in *Biotechnol,* Vol 8 (Edited by W. Shonborn), pp. 425-452. VCH Verlagsgesellschaft, Wienheim, Germany.

Ottengraf , S. P. P. and Diks, R., 1990, Biological purification of waste gases, *Chimicaoggi*, May, p41.

Ottengraf , S. P. P.,Meesters, J. J. P., van den Oever,A. H. C.and Rozema H.R., 1986, Biological elimination of volatile xenobiotic compounds in biofilters, *Bioprocess Eng.* vol 1, p 61.

Ottengraf , S. P. P. and van den Oever,A. H. C., 1983, Kinetics of organic compound removal from waste gases with a biological filter, *Biotechnol. Bioenng* 25, p 3089.

Ottengraf , S. P. P., van den Oever,A. H. C. and Kempenaars, F. J. C. M., 1983, Waste gas purification in a biological filter bed, In : *Innovations in Biotechnology*, Elsvier Science Publications, Amsterdam.

Phipps Jr., D. W. and Ridgeway, H. F., 1993, Modular bioreactor and computerized instrumentation package to identify critical design parameters for vapor phase bioreators, Proceedings of the 2nd International Symposium on In Situ and On-Site bioreclamation, San Diego, CA.

Perry, R. H. and Green, D., 1984, *Perry's Chemical Engineers' Handbook*, 6th edition. McGraw Hill, NewYork, NY.

Ruthven, D. M., 1984, *Principles of Adsorption and Adsorption Processes*, pp 134-135, pp 206-213, John Wiley & Sons.

Sorial, G. A., Smith, F. L., Suidan, M. T. and Biswas, P, 1993, Development of aerobic biofilter design criteriafor treating VOCs, in Proceedings of the 86h A& WMA meeting, Paper No. 93-TP-52A.04, Air & Waste Management Association, Denver, CO.

Swaine, D. E. and Daugulis, A.J., 1988, Review of liquid mixing in packed bed biological reactors. *Biotechnol. Prog.*, vol 4, no 3, p 134.

Togna, A. P. and Singh, M., 1994, Biological vapor phase treatment using biofilter and biotrickling filter reactors : practical operating regimes. *Environmental. Progress.*, vol 13, no 2, p 94.

Torres, E. M., Basrai, S., Carlson, S., Gosette, R., Kogan, V., Devinny, J., Mi, Y., Webster, T. and Stolin, B., Study of biofiltration for control of VOC & Toxic

emissions from waste water treatment plants, in Proceedings of the 87th A& WMA meeting, Paper No. 94-WP92, Air & Waste Management Association, Cincinatti, Ohio.

Van Lith, C., David, S.L.and Marsh, R., 1990, Design criteria for biofilters, *Trans IChemE.* 68, p127.

Zarook, S., 1994, Engineering analysis of a packed-bed biofilter for removal of volatile organic compound (VOC) emissions. Ph.D. thesis, New Jersey Institute of Technology, Newark, NJ.

Zarook, S., Baltzis, B. C., Oh, Y. S. and Bartha, R., 1991, Biofiltration of methanol vapor. *Biotechnol. Bioenng.* 41, p 512.

Zarook, S.and Baltzis, B. C., 1994, Biofiltration of toluene vapor under steady-state and transient conditions: Theory and experimental results, *Chemical Engineering Science*, 49, p 4347.

Zilli, M., Converti, A., Lodi, A., Del Borghi, M. and Ferraiol G., 1993, Phenol removal from waste gases with biological filter by *Pseudomonas putida. Biotechnol. Bioenng* 41, p 693.

APPENDIX A

Residence Time Distribution Experiments

RUN 2			RUN 3			RUN 4	
Time	Conc.		Time	Conc.		Time	Conc.
(min)	(g m^{-3})		(min)	(g m^{-3})		(min)	(g m^{-3})
0	0		0	0		0	0
9	0.662		17	4.144		10	0.248
14	2.602		26	11.86		15	0.338
18	4.773		35	3.635		25	1.248
28	5.249		40	2.537		30	2.314
33	4.557		45	1.181		35	3.464
38	3.001		51	1.165		40	4.011
43	2.106		56	0.89		50	8.032
48	1.673		65	0.639		55	12.39
52	1.351		79	0.309		60	15.11
63	1.167		84	0.005		65	16.71
68	1.097		102	0.002		77	13.67
77	0.721					82	9.936
						86	7.909
						96	5.383
						122	6.306
						128	6.309
						175	6.278
						203	6.301
						208	6.091
						217	6.369

C(θ) Curves obtained experimentally

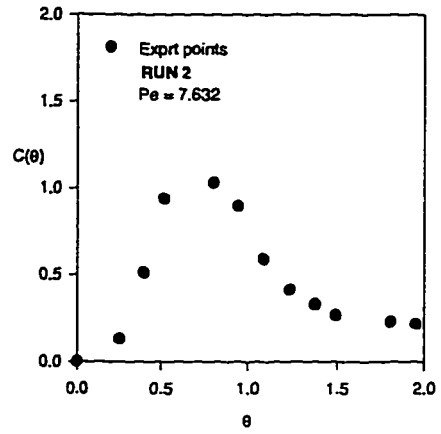

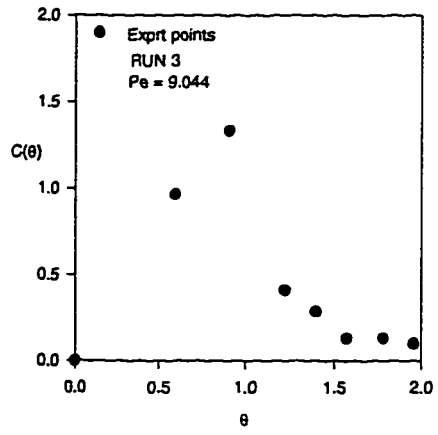

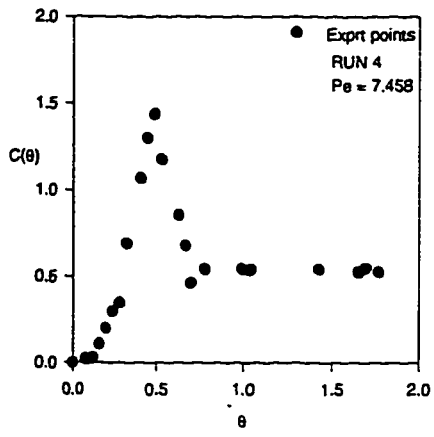

APPENDIX B

Experimental Data on Biofiltration of TolueneVapor

C_{TI} = 1.5 g/m^3; Flow rate= 1.008 L/min; τ = 2.03 mins; x_{H2O} = 30%, O_2 = 21% (air)

Transient Data

Time (days)	Inlet Conc. (g/m^3)	Time (days)	Port1 (g/m^3)	Time (days)	Port2 (g/m^3)	Time (days)	Port3 (g/m^3)	Time (days)	Port4 (g/m^3)	Time (days)	Exit Conc. (g/m^3)
0.25	1.207	0.25195	1.118	0.2539	1.046	0.25585	1.003	0.2578	0.996	0.25975	0.975
0.625	1.323	0.62695	1.214	0.6289	1.169	0.63085	1.083	0.6328	1.005	0.63475	0.986
1	1.567	1.00195	1.406	1.0039	1.325	1.00585	1.228	1.0078	1.106	1.00975	0.993
1.5	1.593	1.50195	1.498	1.5039	1.416	1.50585	1.309	1.5078	1.213	1.50975	1.105
2	1.573	2.00195	1.463	2.0039	1.394	2.00585	1.267	2.0078	1.115	2.00975	1.003
2.33	1.559	2.33195	1.293	2.3339	1.046	2.33585	0.963	2.3378	0.893	2.33975	0.604
2.65	1.613	2.65195	1.432	2.6539	1.278	2.65585	1.143	2.6578	0.987	2.65975	0.801
3	1.551	3.00195	1.286	3.0039	1.105	3.00585	0.952	3.0078	0.824	3.00975	0.621
3.4	1.567	3.40195	1.405	3.4039	1.26	3.40585	1.163	3.4078	1.014	3.40975	0.887

Steady State Data

Dimensionless Distance	Conc. of toluene (g/m^3)
0	1.5
0.2	1.35
0.4	1.17
0.6	1.05
0.8	0.93
1	0.72

Dimensionless Distance	Dimensionless Conc. (oxygen)
0	1
0.2	0.997
0.4	0.9965
0.6	0.9958
0.8	0.9943
1	0.99

C_{Ti} = 1.5 g/m^3; Flow rate= 1.008 L/min; τ = 2.03 mins; x_{H2O} = 30%, O_2 = 33%

Transient Data

Time (days)	Inlet Conc. (g/m^3)	Time (days)	Port1 (g/m^3)	Time (days)	Port2 (g/m^3)	Time (days)	Port3 (g/m^3)	Time (days)	Port4 (g/m^3)	Time (days)	Exit Conc. (g/m^3)
0.25	1.234	0.25195	1.216	0.2539	1.185	0.25585	1.105	0.2578	1.008	0.25975	0.792
0.635	1.356	0.63695	1.304	0.6389	1.253	0.64085	1.192	0.6428	1.094	0.64475	0.904
1.325	1.492	1.32695	1.425	1.3289	1.408	1.33085	1.203	1.3328	1.113	1.33475	0.915
1.65	1.534	1.65195	1.519	1.6539	1.451	1.65585	1.183	1.6578	1.107	1.65975	0.82
1.85	1.569	1.85195	1.512	1.8539	1.406	1.85585	1.114	1.8578	1.052	1.85975	0.856
2	1.526	2.00195	1.5	2.0039	1.301	2.00585	1.0846	2.0078	0.91	2.00975	0.693
2.54	1.481	2.54195	1.382	2.5439	1.16	2.54585	0.912	2.5478	0.82	2.54975	0.657
3	1.513	3.00195	1.495	3.0039	1.26	3.00585	1.046	3.0078	0.956	3.00975	0.694
3.5	1.504	3.50195	1.401	3.5039	1.08	3.50585	0.9565	3.5078	0.807	3.50975	0.612

Steady State Data

Dimensionless Distance	Conc. of toluene (g/m^3)
0	1.5
0.2	1.443
0.4	1.2
0.6	1.005
0.8	0.87
1	0.66

Dimensionless Distance	Dimensionless Conc. (oxygen)
0	1
0.2	0.998
0.4	0.9973
0.6	0.9962
0.8	0.995
1	0.992

C_{Ti} = 1.5g/m^3; Flow rate= 1.008 L/min; τ = 2.03 mins; x_{H2O} = 50%, O_2 = 21% (air)

Transient Data

Time (days)	Inlet Conc. (g/m^3)	Time (days)	Port1 (g/m^3)	Time (days)	Port2 (g/m^3)	Time (days)	Port3 (g/m^3)	Time (days)	Port4 (g/m^3)	Time (days)	Exit Conc. (g/m^3)
0.333	1.363	0.33495	0.562	0.3369	0.3443	0.33885	0.343	0.3408	0.22	0.34275	0.125
0.625	1.589	0.62695	1.061	0.6289	0.755	0.63085	0.589	0.6328	0.6328	0.63475	0.3188
1	1.796	1.00195	1.303	1.0039	1.011	1.00585	0.653	1.0078	0.486	1.00975	0.427
1.33	1.363	1.33195	0.983	1.3339	0.626	1.33585	0.418	1.3378	0.319	1.33975	0.179
1.625	1.619	1.62695	1.263	1.6289	1.039	1.63085	0.927	1.6328	0.767	1.63475	0.659
2.167	1.496	2.16895	1.091	2.1709	0.858	2.17285	0.73	2.1748	0.582	2.17675	0.425
2.5	1.581	2.50195	1.239	2.5039	0.98	2.50585	0.872	2.5078	0.638	2.50975	0.541
2.8	1.498	2.80195	1.075	2.8039	0.84	2.80585	0.6454	2.8078	0.5123	2.80975	0.442
3.1	1.5016	3.10195	1.1021	3.1039	0.8725	3.10585	0.7251	3.1078	0.5735	3.10975	0.4317
3.5	1.4991	3.50195	1.0316	3.5039	0.8341	3.50585	0.6631	3.5078	0.5261	3.50975	0.4391

Steady State Data

Dimensionless Distance	Conc. (g/m^3)
0	1.5
0.2	1.18875
0.4	0.8625
0.6	0.678
0.8	0.537
1	0.43

C_{Ti} = 1.5 g/m^3; Flow rate= 1.008 L/min; τ = 2.03 mins; x_{H2O} = 30%, O_2 = 53%

Transient Data

Time (days)	Inlet Conc. (g/m^3)	Time (days)	Port1 (g/m^3)	Time (days)	Port2 (g/m^3)	Time (days)	Port3 (g/m^3)	Time (days)	Port4 (g/m^3)	Time (days)	Exit Conc. (g/m^3)
0.156	1.258	0.15795	1.156	0.1599	0.962	0.16185	0.815	0.1638	0.673	0.16575	0.486
0.5	1.39	0.50195	1.294	0.5039	1.107	0.50585	1.005	0.5078	0.961	0.50975	0.681
1	1.457	1.00195	1.386	1.0039	1.153	1.00585	1.108	1.0078	1.002	1.00975	0.643
1.33	1.574	1.33195	1.486	1.3339	1.216	1.33585	1.143	1.3378	1.076	1.33975	0.685
1.625	1.538	1.62695	1.465	1.6289	1.115	1.63085	1.008	1.6328	0.91	1.63475	0.681
2	1.482	2.00195	1.423	2.0039	1.131	2.00585	1.002	2.0078	0.887	2.00975	0.667
2.625	1.536	2.62695	1.394	2.6289	1.015	2.63085	0.912	2.6328	0.729	2.63475	0.574
3.25	1.514	3.25195	1.45	3.2539	1.115	3.25585	0.986	3.2578	0.851	3.25975	0.612
3.75	1.495	3.75195	1.379	3.7539	0.997	3.75585	0.831	3.7578	0.715	3.75975	0.583

Steady State Data

Dimensionless Distance	Conc. of toluene (g/m^3)
0	1.5
0.2	1.41
0.4	1.065
0.6	0.93
0.8	0.795
1	0.57

Dimensionless Distance	Dimensionless Conc. (oxygen)
0	1
0.2	0.995
0.4	0.99
0.6	0.982
0.8	0.975
1	0.972

C_{TI} = 1.5g/m^3; Flow rate= 1.008 L/min; τ = 2.03 mins; x_{H2O} = 70%, O_2 = 21% (air)

Transient Data

Time (days)	Inlet Conc. (g/m^3)	Time (days)	Port1 (g/m^3)	Time (days)	Port2 (g/m^3)	Time (days)	Port3 (g/m^3)	Time (days)	Port4 (g/m^3)	Time (days)	Exit Conc. (g/m^3)
0.33	1.519	0.33195	1.409	0.3339	1.067	0.33585	0.933	0.3378	0.779	0.33975	0.648
0.67	1.55	0.67195	1.484	0.6739	1.0976	0.67585	0.965	0.6778	0.743	0.67975	0.532
1	1.5025	1.00195	1.3	1.0039	1.012	1.00585	0.854	1.0078	0.633	1.00975	0.519
1.33	1.6216	1.3319	1.5237	1.334	1.1864	1.336	1.021	1.338	0.7562	1.34	0.5752
1.67	1.5108	1.672	1.1564	1.674	0.9002	1.676	0.8587	1.678	0.6865	1.68	0.4365
2.35	1.55	2.352	1.3063	2.354	1.16	2.356	0.8946	2.358	0.5482	2.36	0.3822
2.75	1.49	2.752	1.18563	2.754	0.9229	2.756	0.7752	2.758	0.5735	2.76	0.41732
3.25	1.5362	3.252	1.2154	3.254	0.9461	3.256	0.7975	3.258	0.5912	3.26	0.404585

Steady State Data

Dimensionless Distance	Conc. (g/m^3)
0	1.5
0.2	1.2
0.4	1.0005
0.6	0.8499
0.8	0.6
1	0.444

C_{TI} = 2.17g/m^3; Flow rate= 1.015 L/min; t = 2.0197 mins; x_{H2O} = 30%, O_2 = 21% (air)

Transient Data

Time (days)	Inlet Conc. (g/m^3)	Time (days)	Port1 (g/m^3)	Time (days)	Port2 (g/m^3)	Time (days)	Port3 (g/m^3)	Time (days)	Port4 (g/m^3)	Time (days)	Exit Conc. (g/m^3)
0	2.170494	0.00195	1.694048	0.0039	1.437841	0.00585	1.214612	0.0078	1.068352	0.00975	0.9173786
0.08625	1.699897	0.0882	1.759225	0.09015	1.347732	0.0921	1.236946	0.09405	0.956859	0.096	0.8289647
0.162917	2.0071616	0.164867	1.72279	0.166817	1.493508	0.168767	1.352202	0.170717	1.074946	0.172667	0.8688362
0.004167	2.2204521	0.006117	1.976399	0.008067	1.730725	0.010017	1.45141	0.011967	1.323721	0.013917	1.0689386
1.125	2.2474801	1.12695	2.1681	1.1289	1.898109	1.13085	1.72442	1.1328	1.449958	1.13475	1.3197815
1.75	1.8197163	1.75195	1.73554	1.7539	1.070075	1.75585	1.270224	1.7578	1.065139	1.75975	0.8499948
2.0833	2.2253324	2.08525	1.992427	2.0872	1.726878	2.08915	1.534935	2.0911	1.225891	2.09305	1.080087
2.70833	2.1557506	2.71028	1.919903	2.71223	1.7814	2.71418	1.563714	2.71613	1.325174	2.71808	1.0396474
3.16666	2.0604353	3.16861	1.874424	3.17056	1.747722	3.17251	1.503241	3.17446	1.29673	3.17641	0.9871187
3.61254	2.1032685	3.61449	1.882779	3.61644	1.729598	3.61839	1.525453	3.62034	1.265595	3.62229	1.0078229
3.83333	2.1351676	3.83528	1.897736	3.83723	1.69253	3.83918	1.522417	3.84113	1.273847	3.84308	0.9737724
4.041678	2.0839521	4.043628	1.893517	4.045578	1.686932	4.047528	1.511669	4.049478	1.250414	4.051428	1.0301382
4.33333	2.097699	4.33528	1.878262	4.33723	1.71749	4.33918	1.53296	4.34113	1.284222	4.34308	0.987333

Steady State Data

Dimensionless Distance	Conc. (g/m^3)
0	2.17
0.2	1.951
0.4	1.775
0.6	1.573
0.8	1.319
1	1.019

C_{TI} = 2.17g/m^3; Flow rate= 1.015 L/min; τ = 2.0197 mins; x_{H2O} = 50%, O_2 = 21% (air)

Transient Data

Time (days)	Inlet Conc. (g/m^3)	Time (days)	Port1 (g/m^3)	Time (days)	Port2 (g/m^3)	Time (days)	Port3 (g/m^3)	Time (days)	Port4 (g/m^3)	Time (days)	Exit Conc. (g/m^3)
0.33	2.256	0.33195	1.658	0.3339	1.144	0.33585	0.9398	0.3378	0.6448	0.33975	0.4581
0.625	2.113	0.62695	1.66	0.6289	1.411	0.63085	1.235	0.6328	0.936	0.63475	0.8555
1	2.142	1.00195	1.629	1.0039	1.4527	1.00585	1.1195	1.0078	0.949	1.00975	0.8379
1.33	2.19	1.33195	1.941	1.3339	1.829	1.33585	1.692	1.3378	1.441	1.33975	1.35
1.65	2.276	1.65195	1.899	1.6539	1.659	1.65585	1.428	1.6578	0.921	1.65975	0.9199
2.167	2.089	2.16895	1.66	2.1709	1.442	2.17285	1.187	2.1748	1.064	2.17675	0.8466
2.75	2.0121	2.75195	1.5	2.7539	1.384	2.75585	1.131	2.7578	0.987	2.75975	0.973
3	2.068	3.00195	1.754	3.0039	1.456	3.00585	1.289	3.0078	1.08	3.00975	0.93
3.5	2.161	3.50195	1.7119	3.5039	1.439	3.50585	1.174	3.5078	1.0294	3.50975	0.85

Steady State Data

Dimensionless Distance	Conc. (g/m^3)
0	2.17
0.2	1.68175
0.4	1.40616
0.6	1.17831
0.8	1.00688
1	0.86366

C_{TI} = 2.17g/m^3; Flow rate= 1.015 L/min; τ = 2.0197 mins; x_{H2O} = 70%, O_2 = 21% (air)

Transient Data

Time (days)	Inlet Conc. (g/m^3)	Time (days)	Port1 (g/m^3)	Time (days)	Port2 (g/m^3)	Time (days)	Port3 (g/m^3)	Time (days)	Port4 (g/m^3)	Time (days)	Exit Conc. (g/m^3)
0.25	2.1	0.25195	1.895	0.2539	1.708	0.25585	1.257	0.2578	1.23	0.25975	1.186
0.54	2.245	0.54195	1.826	0.5439	1.652	0.54585	1.2	0.5478	1.172	0.54975	1.12
0.821	2.153	0.82295	1.716	0.8249	1.61	0.82685	1.164	0.8288	1.13	0.83075	0.952
1.25	2.18	1.25195	1.657	1.2539	1.498	1.25585	1.015	1.2578	1.01	1.25975	0.816
1.75	2.282	1.75195	1.742	1.7539	1.55	1.75585	1.124	1.7578	1.1	1.75975	0.85
2.135	2.215	2.13695	1.713	2.1389	1.51	2.14085	1.0901	2.1428	1.058	2.14475	0.832
2.513	2.1	2.51495	1.736	2.5169	1.534	2.51885	1.0799	2.5208	1.035	2.52275	0.89
3	2.16	3.00195	1.845	3.0039	1.496	3.00585	1.062	3.0078	1.0652	3.00975	0.935
3.25	2.18	3.25195	1.702	3.2539	1.54	3.25585	1.12	3.2578	1.021	3.25975	0.862

Steady State Data

Dimensionless Distance	Conc. (g/m^3)
0	2.17
0.2	1.740557
0.4	1.522038
0.6	1.088906
0.8	1.047242
1	0.8897

C_{Ti} = 3.0g/m^3; Flow rate = 1.03 L/mins; τ = 1.99 mins; x_{H2O} = 30%, O_2 = 21% (air)

Transient Data

Time	Inlet	Time	Port1	Time	Port2	Time	Port3	Time	Port4	Time	Exit
0	3.06363	0.00195	2.569926	0.0039	2.167216	0.00585	1.912992	0.0078	1.767691	0.00975	1.686597
0.144	3.371714	0.14595	2.539144	0.1479	1.747173	0.14985	1.552323	0.1518	1.315022	0.15375	1.453059
1.034	2.920592	1.03595	2.619605	1.0379	2.355331	1.03985	2.202225	1.0418	2.186821	1.04375	1.849678
1.15	2.873092	1.15195	2.524839	1.1539	2.394709	1.15585	2.24097	1.1578	1.949566	1.15975	1.799171
2.09325	2.913197	2.0952	2.642311	2.09715	2.392427	2.0991	2.200735	2.10105	1.900111	2.103	1.829496
2.29587	2.954288	2.29782	2.687473	2.29977	2.47217	2.30172	2.25657	2.30367	2.167979	2.30562	1.891897
2.42625	2.933286	2.4282	2.667439	2.43015	2.432672	2.4321	2.221234	2.43405	2.01179	2.436	1.855359
2.97708	2.944621	2.97903	2.657166	2.98098	2.45183	2.98293	2.237403	2.98488	2.125435	2.98683	1.815376
3.06451	2.958973	3.06646	2.675132	3.06841	2.428052	3.07036	2.198984	3.07231	2.06078	3.07426	1.837412

Steady State Data

Dimensionless Distance	Conc. (g/m$_3$)
0	3
0.2	2.724
0.4	2.487
0.6	2.268
0.8	2.127
1	1.87

C_{Ti} = 4.026 g/m^3 ; Flow rate = 1.045 lt/min ; τ = 1.96 min; x_{H2O} = 30%; O_2 = 21% (air)

Transient Data

Time (days)	Inlet Conc. (g/m^3)	Time (days)	Port1 (g/m^3)	Time (days)	Port2 (g/m^3)	Time (days)	Port3 (g/m^3)	Time (days)	Port4 (g/m^3)	Time (days)	Exit Conc. (g/m^3)
0	3.3878825	0.003	3.448309	0.00625	3.344546	11.08	3.08629	0.0125	2.602048	0.0152	2.0792581
0.101375	3.4295887	0.104375	3.524941	0.106875	3.231302	0.109705	2.337552	0.114565	2.34083	0.117275	1.8621676
0.3513	4.3337705	0.3543	3.845412	0.35616	3.674862	0.36757	3.395678	0.3637	2.932616	0.36654	2.0516526
1.0833	3.9676999	1.0863	3.573474	1.08955	3.428275	1.0937	3.253329	1.09857	2.632951	1.10134	1.4404204
1.270833	3.8824061	1.273833	3.087556	1.2768	2.842376	1.28569	2.542767	1.28958	1.975486	1.29653	1.3050847
2.20125	4.5730739	2.2045	3.925817	2.2645	3.586271	2.2978	3.321775	2.30145	2.609378	2.35145	2.4323548
3.2825	4.0753277	3.2855	3.608987	3.2907	3.316196	3.29897	3.036034	3.30145	2.697438	3.356781	2.2542045
4.24236	4.153329	4.24536	3.494402	4.29632	3.335391	4.30186	3.001266	4.36785	2.662689	4.39548	2.2326995

Steady State Data

Dimensionless Distance	Conc. (g/m^3)
0	4.026
0.2	3.467
0.4	3.216
0.6	2.941
0.8	2.517
1	2.14

C_{TI} = 10 g/m^3; Flow rate= 2.1 L/min; τ = 0.976 mins; x_{H2O} = 30%, O_2 = 21% (air)

Transient Data

Time (days)	Inlet Conc. (g/m^3)	Time (days)	Port1 (g/m^3)	Time (days)	Port2 (g/m^3)	Time (days)	Port3 (g/m^3)	Time (days)	Port4 (g/m^3)	Time (days)	Exit Conc. (g/m^3)
0.325	10.60738	0.32695	9.584	0.3289	9.435	0.33085	9.409	0.3328	9.384	0.33475	9.257
0.75	9.810133	0.75195	9.628	0.7539	9.616	0.75585	9.586	0.7578	9.567	0.75975	9.392
1.265	10.15186	1.26695	9.832	1.2689	9.804	1.27085	9.761	1.2728	9.703	1.27475	9.531
1.675	10.01795	1.67695	9.761	1.6789	9.716	1.68085	9.683	1.6828	9.625	1.68475	9.503
2	10.15129	2.00195	9.852	2.0039	9.749	2.00585	9.664	2.0078	9.608	2.00975	9.463
2.33	9.480441	2.33195	9.376	2.3339	9.315	2.33585	9.293	2.3378	9.258	2.33975	9.192
2.5	9.875216	2.50195	9.768	2.5039	9.714	2.50585	9.352	2.5078	9.293	2.50975	9.019
2.765	9.975489	2.76695	9.812	2.7689	9.763	2.77085	9.638	2.7728	9.504	2.77475	9.201
3.25	10.0325	3.25195	9.793	3.2539	9.641	3.25585	9.435	3.2578	9.382	3.25975	9.037
3.65	9.9853	3.65195	9.861	3.6539	9.69	3.65585	9.602	3.6578	9.473	3.65975	9.152

Steady State Data

Dimensionless Distance	Conc. of toluene (g/m^3)	Dimensionless Distance	Dimensionless Conc. (oxygen)
0	10	0	1
0.2	9.8	0.2	0.996
0.4	9.7	0.4	0.994
0.6	9.5	0.6	0.9928
0.8	9.4	0.8	0.991
1	9.1	1	0.983

C_{Ti} = 10 g/m^3; Flow rate= 2.1 L/min; τ = 0.976 mins; x_{H2O} = 30%, O_2 = 100%

Transient Data

Time (days)	Inlet Conc. (g/m^3)	Time (days)	Port1 (g/m^3)	Time (days)	Port2 (g/m^3)	Time (days)	Port3 (g/m^3)	Time (days)	Port4 (g/m^3)	Time (days)	Exit Conc. (g/m^3)
0.208	9.77	0.20995	9.149	0.2119	8.81	0.21385	8.53	0.2158	8.37	0.21775	8.264
0.507	9.548	0.50895	9.254	0.5109	8.779	0.51285	8.84	0.5148	8.652	0.51675	8.44
0.75	10.486	0.75195	9.9216	0.7539	9.8	0.75585	9.673	0.7578	9.57	0.75975	9.378
1	9.952	1.00195	9.7959	1.0039	9.514	1.00585	9.17	1.0078	9.046	1.00975	8.835
1.326	9.532	1.32795	8.952	1.3299	8.78	1.33185	8.685	1.3338	8.56	1.33575	8.43
1.75	9.8623	1.75195	9.2	1.7539	9.02	1.75585	8.74	1.7578	8.259	1.75975	8.09
2.25	10.12	2.25195	9.609	2.2539	9.26	2.25585	9.05	2.2578	8.901	2.25975	8.49
2.675	9.9482	2.67695	9.82	2.6789	9.23	2.68085	8.81	2.6828	8.765	2.68475	8.41
3	9.857	3.00195	9.532	3.0039	9.327	3.00585	9.26	3.0078	9.013	3.00975	8.6
3.5	10.25	3.50195	9.61	3.5039	8.983	3.50585	8.91	3.5078	8.65	3.50975	8.326

Steady State Data

Dimensionless Distance	Conc. of toluene (g/m^3)	Dimensionless Distance	Dimensionless Conc. (oxygen)
0	10	0	1
0.2	9.57	0.2	0.9985
0.4	9.2	0.4	0.998
0.6	9	0.6	0.9973
0.8	8.8	0.8	0.9962
1	8.43	1	0.996

C_{TI} =17.5g/m^3; Flow rate= 2.6 L/min; τ = 0.785 mins; x_{H2O} = 30%, O_2 = 21% (air)

Transient Data

Time (days)	Inlet Conc. (g/m^3)	Time (days)	Port1 (g/m^3)	Time (days)	Port2 (g/m^3)	Time (days)	Port3 (g/m^3)	Time (days)	Port4 (g/m^3)	Time (days)	Exit Conc. (g/m^3)
0.167	17.3	0.16895	16.89	0.1709	16.69	0.17285	16.65	0.1748	16.439	0.17675	16.37
0.5	17.45	0.50195	17.19	0.5039	16.95	0.50585	16.82	0.5078	16.66	0.50975	16.58
1	16.85	1.00195	16.526	1.0039	16.265	1.00585	15.6262	1.0078	16.126	1.00975	15.93
1.5	17.58	1.50195	16.66	1.5039	16.97	1.50585	16.93	1.5078	16.56	1.50975	16.79
2	17.55	2.00195	17.55	2.0039	17.19	2.00585	16.46	2.0078	15.5	2.00975	15.125
2.33	18.8	2.33195	17.58	2.3339	17.16	2.33585	17.32	2.3378	16.74	2.33975	16.41
2.677	17.5	2.67895	17.46	2.6809	17.3	2.68285	17.2	2.6848	16.789	2.68675	16.19
3	17.7	3.00195	17.63	3.004	17.43	3.006	17.4	3.009	16.623	3.01	16.45
3.33	17.2	3.332	17.15	3.334	17.01	3.336	17.023	3.338	16.34	3.34	16.23
3.625	17.5	3.627	17.42	3.629	17.15	3.631	17.12	3.633	16.75	3.635	16.6

Steady State Data

Dimensionless Distance	Conc. of toluene (g/m^3)	Dimensionless Distance	Dimensionless Conc. (oxygen)
0	17.5	0	1
0.2	17.38	0.2	0.997
0.4	17.22	0.4	0.9961
0.6	17.08	0.6	0.9954
0.8	16.66	0.8	0.993
1	16.44	1	0.9926

C_{TI} = 17.5 g/m^3; Flow rate= 2.6 L/min; τ = 0.785 mins; x_{H2O} = 30%, O_2 = 53%

Transient Data

Time (days)	Inlet Conc. (g/m^3)	Time (days)	Port1 (g/m^3)	Time (days)	Port2 (g/m^3)	Time (days)	Port3 (g/m^3)	Time (days)	Port4 (g/m^3)	Time (days)	Exit Conc. (g/m^3)
0.5	16.76	0.502	16.64	0.5039	16.453	0.5059	16.306	0.5078	16.264	0.5098	16.108
0.85	17.465	0.852	17.325	0.8539	17.207	0.8559	17.153	0.8578	17.096	0.8598	16.853
1.33	17.9	1.332	17.764	1.3339	17.683	1.3359	17.539	1.3378	17.394	1.3398	17.197
1.675	17.02	1.677	16.947	1.6789	16.873	1.6809	16.807	1.6828	16.783	1.6848	16.703
2	17.57	2.0019	17.462	2.0039	17.415	2.0058	17.264	2.0078	17.158	2.0097	16.998
2.33	17.94	2.3319	17.79	2.3339	17.652	2.3358	17.408	2.3378	17.293	2.3397	17.106
2.5	17.83	2.5019	17.384	2.5039	17.014	2.5058	16.904	2.5078	16.307	2.5097	16.013
2.85	17.46	2.8519	17.214	2.8539	17.106	2.8558	17.038	2.8578	16.56	2.8597	16.289
3.335	17.35	3.337	17.253	3.3389	16.941	3.3408	16.77	3.3428	16.352	3.3447	16.043
3.765	17.56	3.767	17.362	3.7689	17.115	3.7708	17.056	3.7728	16.601	3.7747	16.215

Steady State Data

Dimensionless Distance	Conc. of toluene (g/m^3)
0	17.5
0.2	17.3075
0.4	17.045
0.6	16.94
0.8	16.45
1	16.135

Dimensionless Distance	Dimensionless Conc. (oxygen)
0	1
0.2	0.998
0.4	0.9972
0.6	0.9963
0.8	0.9957
1	0.9946

C_{TI} = 17.5g/m^3; Flow rate= 2.6 L/min; τ = 0.785 mins; x_{H2O} = 30%, O_2 = 100%

Transient Data

Time (days)	Inlet Conc. (g/m^3)	Time (days)	Port1 (g/m^3)	Time (days)	Port2 (g/m^3)	Time (days)	Port3 (g/m^3)	Time (days)	Port4 (g/m^3)	Time (days)	Exit Conc. (g/m^3)
0.5	19.52	0.502	19.396	0.5039	19.29	0.5059	18.91	0.5078	18.83	0.5098	18.78
0.85	18.15	0.852	17.23	0.8539	17.38	0.8559	15.74	0.8578	16.8	0.8598	17.43
1.33	18.79	1.332	17.75	1.3339	16.53	1.3359	16.179	1.3378	12.428	1.3398	16.511
1.675	17.006	1.677	16.44	1.6789	16.15	1.6809	15.99	1.6828	16.099	1.6848	16.06
2	17.379	2.0019	17.33	2.0039	17.04	2.0058	16.94	2.0078	16.8	2.0097	16
2.33	17.18	2.3319	16.95	2.3339	17.18	2.3358	16.06	2.3378	15.87	2.3397	16.05
2.5	17.44	2.5019	17.32	2.5039	17.22	2.5058	16.865	2.5078	16.5281	2.5097	16.2465
2.85	17.73	2.8519	18.14	2.8539	17.3	2.8558	16.5123	2.8578	16.8625	2.8597	16.1492
3.335	17.45	3.337	17.246	3.3389	17.102	3.3408	17.012	3.3428	16.452	3.3447	16.3512
3.765	17.61	3.767	17.325	3.7689	17.256	3.7708	16.9247	3.7728	16.3516	3.7747	16.1056

Steady State Data

Dimensionless Distance	Conc. (g/m^3)
0	17.5
0.2	17.15
0.4	17.01
0.6	16.76675
0.8	16.3415
1	16.0545

Dimensionless Distance	Dimensionless Conc. (oxygen)
0	1
0.2	0.9992
0.4	0.9982
0.6	0.9971
0.8	0.9965
1	0.996

APPENDIX C

Discretization of Model Equations by Orthogonal Collocation

Orthogonal collocation formulation

The model equations given in chapter 3 have been solved by using the method of orthogonal collocation. This method reduces the ordinary differential equation to non-linear algebraic equations. The respective orthogonal collocation formulation has been written below after each dimensionless equations.

Pollutant in gas phase

At $Z = 0$

$$\frac{1}{Pe}\frac{\partial \overline{C}_j}{\partial h} = \overline{C}_j - 1 \tag{1}$$

I = 1

$$\frac{1}{Pe}\sum_{K=1}^{M+2} A(1,K)C(K) - C(1) + 1 = 0 \tag{2}$$

$$\frac{1}{Pe}\frac{\partial^2 \overline{C}_j}{\partial Z^2} - \frac{\partial \overline{C}_j}{\partial Z} + \eta \left.\frac{\partial \overline{S}_j}{\partial \theta}\right|_{\theta = 0} = 0 \tag{3}$$

I = 2, M+1

$$\frac{1}{Pe}\sum_{K=1}^{M+2} B(I,K)\, C(K) - \sum_{K=1}^{M+2} A(I,K)\, C(K) +$$

$$\eta \sum_{L=1}^{N+2} AA(1,L)\, C(I + (L+1) * (M+2)) = 0 \tag{4}$$

At $Z = 1$

$$\frac{\partial \overline{C}_j}{\partial Z} = 0 \tag{5}$$

I = M+2

$$\sum_{K=1}^{M+2} A(M+2,K)\ C(K)\ =\ 0 \tag{6}$$

Oxygen in gas phase

At $Z\ =\ 0$

$$\frac{1}{Pe}\frac{\partial \overline{C}_o}{\partial h}\ =\ \overline{C}_o\ -\ 1 \tag{7}$$

I = 1

$$\frac{1}{Pe}\sum_{K=1}^{M+2} A(1,K)\ C(K+(M+2)) - C(1+(M+2))+1\ =\ 0 \tag{8}$$

$$\frac{1}{Pe}\frac{\partial^2 \overline{C}_o}{\partial Z^2}\ -\ \frac{\partial \overline{C}_o}{\partial Z}\ +\ \eta\,\omega\ \left.\frac{\partial \overline{S}_o}{\partial \theta}\right|_{\theta\ =\ 0}\ =\ 0 \tag{9}$$

I = 2, M+1

$$\frac{1}{Pe}\sum_{K=1}^{M+2} B(I,K)\ C(K+(M+2))\ -\ \sum_{K=1}^{M+2} A(I,K)\ C(K+(M+2))$$

$$+\ \eta\,\omega\sum_{L=1}^{N+2} AA(1,L)\ C(I+(L+1)*(M+2)+(M+2)*(N+2))\ =\ 0 \tag{10}$$

At $Z\ =\ 1$

$$\frac{\partial \overline{C}_o}{\partial Z}\ =\ 0 \tag{11}$$

I = M+2

$$\sum_{K=1}^{M+2} A(M+2,K)\ C(K+(M+2))\ =\ 0 \tag{12}$$

Pollutant in biofilm

At $\theta = 0$,

$$\overline{S}_j = \varepsilon_1 \overline{C}_j \tag{13}$$

I = 1, M+2

$$C(I + 2 * (M + 2)) - \varepsilon 1 \; C(I) = 0 \tag{14}$$

$$\frac{\partial^2 \overline{S}_j}{\partial \theta^2} - \Phi^2 \frac{\overline{S}_j}{1 + \overline{S}_j + \gamma \overline{S}_j^2} \frac{\overline{S}_o}{1 + \overline{S}_o} = 0 \tag{15}$$

I = 1, M+2 and

J = 2, N+1

$$\sum_{K=1}^{N+2} BB(J,K) \; C(I + (K+1) * (M+2)) -$$

$$\phi^2 \frac{C(I + (J+1) * (M+2))}{[1 + C(I + (J+1) * (M+2)) + \gamma [C(I + (J+1) * (M+2))]^2]} *$$

$$\frac{C(I + (J+1) * (M+2) + (N+2) * (M+2))}{[1 + C(I + (J+1) * (M+2) + (N+2) * (M+2))]} = 0 \tag{16}$$

At $\theta = 1$,

$$\frac{d\overline{S}_j}{d\theta} = 0 \tag{17}$$

I = 1, M+2

$$\sum_{K=1}^{N+2} AA(N+2,K) \; C(I + (K+1) * (M+2)) = 0 \tag{18}$$

Oxygen in biofilm

At $\theta = 0$,

$$\overline{S}_o = \varepsilon_2 \overline{C}_o \tag{19}$$

I = 1, M+2

$$C(I + 2 * (M + 2) + (N + 2) * (M + 2)) - \varepsilon 2\, C(I + (M + 2)) = 0 \tag{20}$$

$$\frac{\partial^2 \overline{S}_o}{\partial \theta^2} - \Phi^2 \lambda \frac{\overline{S}_j}{1 + \overline{S}_j + \gamma \overline{S}_j^2} \frac{\overline{S}_o}{1 + \overline{S}_o} = 0 \tag{21}$$

I = 1, M+2 and

J = 2, N+1

$$\sum_{K=1}^{N+2} BB(J,K)\, C(I + (K + 1) * (M + 2) + (N + 2) * (M + 2)) -$$

$$\phi^2 \lambda \frac{C(I + (J + 1) * (M + 2))}{[1 + C(I + (J + 1) * (M + 2)) + \gamma [C(I + (J + 1) * (M + 2))]^2]} *$$

$$\frac{C(I + (J + 1) * (M + 2) + (N + 2) * (M + 2))}{[1 + C(I + (J + 1) * (M + 2) + (N + 2) * (M + 2))]} = 0 \tag{22}$$

At $\theta = 1$,

$$\frac{d\overline{S}_o}{d\theta} = 0 \tag{23}$$

I = 1, M+2

$$\sum_{K=1}^{N+2} AA(N + 2, K)\, C(I + (K + 1) * (M + 2) + (N + 2) * (M + 2)) = 0 \tag{24}$$

APPENDIX D

Computer Code

"STEADY STATE BIOFILTRATION OF TOLUENE"

```
      PARAMETER (M=5,N=8)
      PARAMETER (NT=(M+2)*((N+2)*2+2))
      IMPLICIT DOUBLE PRECISION (A-H,O-Z)
      DOUBLE PRECISION C(NT),A(M+2,M+2),B(M+2,M+2),
     . AA(N+2,N+2),BB(N+2,N+2),Y(M+2),X(N+2),CGUESS(NT)
C
      COMMON A,B,AA,BB,PE,OMEGA,ALAMDA,GAMMA,E1,E2,PHI,EITA
C
      EXTERNAL FCN,DNEQNF

      OPEN (UNIT=4,FILE='C:\SMA\SSTINPT.DAT',STATUS='OLD')
      OPEN(UNIT=11,FILE='C:\SMA\COMP.DAT',STATUS='UNKNOWN')
      OPEN(UNIT=12,FILE='C:\SMA\OXY.DAT',STATUS='UNKNOWN')
      OPEN(UNIT=13,FILE='C:\SMA\BCOMP.DAT',STATUS='UNKNOWN')
      OPEN(UNIT=14,FILE='C:\SMA\BOXY.DAT',STATUS='UNKNOWN')
C-------------------READING ORTHO COLLO PTS----------
      DO 4 I=1,N+2
    4 READ (4,*) X(I)
C
      DO 5 I=1,N+2
      DO 5 J=1,N+2
    5 READ (4,*) AA(I,J)
C
      DO 6 I=1,N+2
      DO 6 J=1,N+2
    6 READ (4,*) BB(I,J)
C
      DO 1 I=1,M+2
    1 READ (4,*) Y(I)
C
      DO 2 I=1,M+2
      DO 2 J=1,M+2
    2 READ (4,*) A(I,J)
C
      DO 3 I=1,M+2
      DO 3 J=1,M+2
    3 READ (4,*) B(I,J)
      DO 710 I=1,NT
  710 CGUESS(I)=0.10
C
```

```
C------------INITIAL GUESS--------------
      E1=0.94
      E2=30.74
      CGUESS(1)=1.0
      CGUESS(1+(M+2))=1.0
      DO 10 I=2,M+2
      CGUESS(I)=0.4
 10   CGUESS(I+(M+2))=1.0
      DO 20 I=1,M+2
      CGUESS(I+2*(M+2))=E1*C(I)
 20   CGUESS(I+2*(M+2)+(N+2)*(M+2))=E2*C(I+(M+2))
      DO 30 I=1,M+2
      DO 30 J=2,N+2
      CGUESS(I+(J+1)*(M+2))=0.2
 30   CGUESS(I+(J+1)*(M+2)+(N+2)*(M+2))=18.0

C-----------------IMSL PARAM-----------------

      ERREL=1E-10
      ITMAX=200

C----------------EFFECTIVE BIOFILM THICKNESS---------
C
      DELTA =17.0E-6
111   DELTA = DELTA+1E-6
      CALL PARAM(OMEGA,GAMMA,ALAMDA,E1,E2,PHI,EITA,
     . DELTA)
      PRINT*, DELTA
      PE=7.53
      CALL DNEQNF(FCN,ERREL,NT,ITMAX,CGUESS,C,FNORM)

C---------------------STABILITY CRITERIA------------

      DO 70 I=1,NT
70    IF (C(I).LT.0.0) C(I)=0.0
      DO 80 I=1,((2+N+2)*(M+2))
80    IF (C(I).GT.1.0) C(I)=1.0
      DO 90 I=(1+(2+N+2)*(M+2)),(((N+2)*2+2)*(M+2))
90    IF (C(I).GT.31.0) C(I)=31.0

      IF (C((M+2)+(N+3)*(M+2)+(N+2)*(M+2)).GT.
     . 0.01*C((M+2)+2*(M+2)+(M+2)*(N+2)).AND.C(1+(N+3)*(M+2)).GT.
     . 0.01*C(1+2*(M+2))) GOTO 111

      CALL SHD (NT,M,N,C,Y,X)
      END
```

```
C-----------------------------PRINTING THE RESULTS-----------------

      SUBROUTINE SHD (NT,M,N,C,Y,X)
      DOUBLE PRECISION C(NT),Y(M+2),X(N+2)

      WRITE(11,6)
C     WRITE(12,6)
C     WRITE(13,6)
C     WRITE(14,6)
6     FORMAT(/,27X,'POINTS',10X,'CONC.',/)
      DO 1000 I=1,M+2
      WRITE(11,5) Y(I),C(I)
      WRITE(12,5) Y(I),C(I+M+2)
      DO 2000 J=1,N+2
2000  WRITE(13,7) X(J),C(I+(J+1)*(M+2)),C(I+(J+1)*(M+2)+(N+2)*(M+2))
C2000  WRITE(14,5) X(J),C(I+(J+1)*(M+2)+(N+2)*(M+2))
5     FORMAT (21X,F14.7,2X,F14.7)
7     FORMAT (1X,F14.7,2(3X,F14.7))
1000  CONTINUE
C      WRITE(11,4) DELTA1
C 4   FORMAT (/,5X,'DELTA =',F6.2,1X,'MICROMETERS',/)
      RETURN
      END

C-----------------------------CALCULATION OF PARAMETERS-----------------

      SUBROUTINE PARAM(OMEGA,GAMMA,ALAMDA,E1,E2,PHI,EITA,
     . DELTA)
      IMPLICIT DOUBLE PRECISION (A-H,O-Z)
C     THE UNITS ARE IN GRAMS,METER,SEC

C ----------------------------MOISTURE CONTENT ------------
       AMOIST=0.3
      ANEW=0.44*(1.0-AMOIST)
      ALPHA=0.65
      H=0.641
      VOLUME=0.00205
      FLOW=.001008
      UG=H*FLOW/VOLUME/60
      FXV=0.195
      DIFFJ=1.03E-9
      SAREA=133.3
      AKJ=11.03
     AKO=0.26
      DIFFO=2.41E-9
      XV=1.0E5
      AMUSTR=4.167E-4
      YJ=0.708
      AKI=78.94
      YOJ=0.341
```

```
      AMJ=0.27
      AMO=34.4

C-----------------------------POLLUTANT & OXYGEN INLET CONC-----
      CJI=1.5
      COI=275.0
C ----------------------------BIOLAYER SURFACE AREA -----

      AS=-242.0*AMOIST-174.0*AMOIST**2.0

      PHI=(XV*AMUSTR*DELTA**2.0/FXV/DIFFJ/AKJ/YJ)
      EITA=FXV*DIFFJ*H*AS*AKJ/UG/CJI/DELTA
      OMEGA=AKO*DIFFO*CJI/AKJ/DIFFJ/COI
      GAMMA=AKJ/AKI
      ALAMDA=DIFFJ*AKJ*YJ/DIFFO/AKO/YOJ
      E1=CJI/AKJ/AMJ
      E2=COI/AKO/AMO

      RETURN
      END
C
C-----------------------------------FCN-------------------
C
      SUBROUTINE FCN(C,ABCC,NT)
      IMPLICIT DOUBLE PRECISION (A-H,O-Z)
      PARAMETER(M=5,N=8)
      DOUBLE PRECISION C(NT),A(M+2,M+2),B(M+2,M+2),
     . AA(N+2,N+2),BB(N+2,N+2),ABCC(NT),SUM(14)

      COMMON A,B,AA,BB,PE,OMEGA,ALAMDA,GAMMA,E1,E2,PHI,EITA

      DO 70 I=2,M+1
      DO 65 J=1,6
65    SUM(J)=0.0
      DO 66 K=1,M+2
      SUM(1)=SUM(1)+B(I,K)*C(K)
      SUM(2)=SUM(2)+A(I,K)*C(K)
      SUM(3)=SUM(3)+B(I,K)*C(K+(M+2))
66    SUM(4)=SUM(4)+A(I,K)*C(K+(M+2))
C
      DO 67 L=1,N+2
C     PRINT *,AA(1,L)
      SUM(5)=SUM(5)+AA(1,L)*C(I+(L+1)*(M+2))
67    SUM(6)=SUM(6)+AA(1,L)*C(I+(L+1)*(M+2)+(N+2)*(M+2))
      ABCC(I)=(SUM(1)/PE-SUM(2)+EITA*SUM(5))
C
70    ABCC(I+(M+2))=(SUM(3)/PE-SUM(4)+EITA*OMEGA*SUM(6))
C
      DO 80 I=1,M+2
```

```
      DO 80 J=2,N+1
      DO 71 K=7,8
71    SUM(K)=0.0
      DO 72 K=1,N+2
      SUM(7)=SUM(7)+BB(J,K)*C(I+(K+1)*(M+2))
72    SUM(8)=SUM(8)+BB(J,K)*C(I+(K+1)*(M+2)+(N+2)*(M+2))
C
      SJ=C(I+(J+1)*(M+2))
      SO=C(I+(J+1)*(M+2)+(N+2)*(M+2))
      ABCC(I+(J+1)*(M+2))=(SUM(7)-PHI*SJ*SO/(1.0+SJ+GAMMA*
     . SJ**2)/(1.0+SO))
80    ABCC(I+(J+1)*(M+2)+(N+2)*(M+2))=(SUM(8)-PHI*ALAMDA*
     . SJ*SO/(1.0+SJ+GAMMA*SJ**2)/(1.0+SO))

      DO 90 I=1,M+2
      ABCC(I+2*(M+2))=(C(I+2*(M+2))-E1*C(I))
      ABCC(I+2*(M+2)+(N+2)*(M+2))=(C(I+2*(M+2)+(N+2)*(M+2))-
     . E2*C(I+(M+2)))
C
      DO 85 K=9,10
85     SUM(K)=0.0
C
      DO 86 K=1,N+2
      SUM(9)=SUM(9)+AA(N+2,K)*C(I+(K+1)*(M+2))
86     SUM(10)=SUM(10)+AA(N+2,K)*C(I+(K+1)*(M+2)+(N+2)*(M+2))

      ABCC(I+(N+3)*(M+2))=SUM(9)
90    ABCC(I+(N+3)*(M+2)+(N+2)*(M+2))=SUM(10)
C
      DO 93 K=11,14
93    SUM(K)=0.0
      DO 95 K=1,M+2
      SUM(11)=SUM(11)+A(1,K)*C(K)
      SUM(12)=SUM(12)+A(1,K)*C(K+(M+2))
      SUM(13)=SUM(13)+A(M+2,K)*C(K)
95    SUM(14)=SUM(14)+A(M+2,K)*C(K+(M+2))
      ABCC(1)=(SUM(11)/PE+1.0-C(1))
      ABCC(1+(M+2))=(SUM(12)/PE+1.0-C(1+(M+2)))
      ABCC(M+2)=SUM(13)
      ABCC(2*(M+2))=SUM(14)
      RETURN
      END
```